RESEARCH MEMORANDUM

INVESTIGATION OF THE LOADS ON A TYPICAL BUBBLE-TYPE CANOPY

By

Bennie W. Cocke, Jr.

Langley Memorial Aeronautical Laboratory
Langley Field, Va.

NATIONAL ADVISORY COMMITTEE
FOR AERONAUTICS

WASHINGTON
July 10, 1947

NACA RM No. L7D07

NATIONAL ADVISORY COMMITTEE FOR AERONAUTICS

RESEARCH MEMORANDUM

INVESTIGATION OF THE LOADS ON A TYPICAL BUBBLE-TYPE CANOPY

By Bennie W. Cocke, Jr.

SUMMARY

In conjunction with a general investigation of aerodynamic forces on cockpit enclosures, surface static pressures have been measured over both the outer and inner surfaces of the conventional single sliding canopy, conventional front and rear sliding canopies, and the bubble-type canopy which are typified by the installations on the Grumman F6F-3, Curtiss SB2C-4E, and Grumman F8F-1 airplanes, respectively. This report presents a preliminary analysis of data obtained for the bubble-type canopy. Plots are presented that show the distribution of pressure at six lateral sections through the canopy for a range of conditions selected to determine the effects of varying canopy position, yaw, power, and lift coefficient. The results indicate that the net aerodynamic loads on the canopy are greatest when the airplane is operating at high speed with the canopy closed. At all altitudes investigated the effect of opening the canopy is to reduce the external-internal pressure differential and therefore, to reduce the exploding forces. Asymmetrical loading is shown for numerous conditions due to propeller operation and airplane yaw but is most extreme at positive yaw attitudes with propeller operating.

right hand prop!

INTRODUCTION

The occurrence of canopy failures on Navy airplanes in flight has indicated that present load requirements used in the design of canopies and their components may not be adequate. The current load requirements are based on wind-tunnel pressure distributions obtained over a range of pitch and yaw attitudes with the canopy closed and do not include accurate measurement of internal pressure or the effects of canopy opening. It is, therefore, desirable that these factors be investigated and the critical load conditions be more accurately defined.

As a result, a general investigation has been conducted at the Langley Laboratory of the National Advisory Committee for Aeronautics to determine the critical load requirements by means of external and

internal pressure measurements on airplanes employing three representative types of canopies. The three types of canopies selected for the tests were the conventional single sliding canopy, conventional front and rear sliding canopies, and the bubble-type canopy which are typified by the installations on the Grumann F6F-3, Curtiss SB2C-4E, and Grumman F8F-1 airplanes, respectively.

As the first phase of the investigation, tests have been made in the Langley full-scale tunnel to determine external and internal pressure distributions on the three types of canopies for an extensive range of simulated flight conditions with canopy position varied from closed to full open.

This report presents the results obtained with the bubble-type canopy on the F8F-1 airplane. Additional reports have been prepared covering results for the conventional single sliding canopy and the conventional front and rear sliding canopies (references 1 and 2).

Airplane

The Grumman F8F-1 airplane is a low-wing, single-place fighter airplane having a wing span of 35 feet 6 inches, a wing area of 244 square feet, and a normal gross weight of 9050 pounds. The airplane is powered by a Pratt & Whitney R-2800-C engine having a propeller to engine gear ratio of 0.45 to 1. The engine has a military power rating of 2100 horsepower at 2800 rpm at sea level. The engine drives a 12-foot 7-inch four-blade Hamilton Standard propeller having H 20C-162-11M5 blades with an activity factor of 106.2. A three-view drawing giving the principal dimensions is shown in figure 1. Figure 2 shows the airplane mounted in the Langley full-scale tunnel.

The cockpit canopy on this airplane consists of a single-piece rearward sliding bubble-type Plexiglas canopy. Photographs showing the canopy arrangement are presented in figure 3. The canopy is equipped with emergency release mechanism so arranged that all points of attachment are released by pulling one center control.

METHODS AND TESTS

Surface static pressures over the exterior of the cockpit canopy were measured by means of flush-type static orifices installed in nine longitudinal rows along the canopy as shown in figure 4. Static pressures at the inner surface of the canopy were measured by means of six 1/16-inch static-pressure tubes installed at locations indicated in figure 4.

The external and internal pressures were measured with propeller removed and with propeller operating and with the canopy set in four positions: namely, closed, 3 inches open, 1/2 open, and full open. For the propeller-removed tests the airplane was set at angles of attack corresponding to lift coefficients of 0.10, 0.50, 0.87, and 1.18 as determined from force-test data (fig. 5). As force-test data were not available for propeller-operating conditions, the angles of attack selected for propeller-removed tests were also used with propeller operating. The lift coefficients for the propeller-operating tests were, therefore, slightly higher than the specified values. Force tests to determine the exact lift coefficients were not justified inasmuch as previous tests (references 1 and 2) had shown that canopy pressures were not appreciably affected by small variations of lift coefficient.

With the propeller removed, the tests included measurements at yawed attitudes of 0° and −7.5° for the two low lift coefficients, and at yaws of −15°, −7.5°, and 0° for the high lift coefficients. Tests were not made at the positive yaw attitudes with the propeller removed as the canopy is symmetrical and the pressures at positive yaw should merely be in the opposite sense from those measured at negative yaw. With the propeller operating, the power-off test procedure was repeated and was extended to include tests for the same series of conditions throughout the corresponding positive yaw range. Thrust coefficients corresponding to constant military power operation in flight for each of the respective lift coefficients were determined from a flight curve of T_c against C_L calculated for sea-level operation with military power (fig. 5).

For all tests with the propeller operating, the propeller was set at a constant blade angle of 18.4° measured at the 0.75-radius station. All data were obtained with cockpit ventilators and cowl flaps closed, and with the tunnel operating at an airspeed of approximately 60 miles per hour.

SYMBOLS

C_L lift coefficient $\left(\frac{L}{q_o S}\right)$

T_c thrust coefficient $\left(\frac{T}{\rho V^2 D^2}\right)$

P pressure coefficient $\left(\frac{p - p_o}{q_o}\right)$

L lift force, pounds

T thrust, pounds

q_o free-stream dynamic pressure, pounds per square foot $\left(\frac{1}{2}\rho V^2\right)$

ρ_o mass density of air, slugs per cubic foot

p local static pressure, pounds per square foot

p_o free-stream static pressure, pounds per square foot

S wing area, square feet

V airspeed, feet per second

D propeller diameter, feet

Subscripts:

i internal

e external

DISCUSSION OF RESULTS

The results of the external pressure measurements are presented in figures 6 to 13 in the form of pressure-distribution plots showing the variation of the external pressure coefficient $\left(\frac{p_e - p_o}{q_o}\right)$ at six lateral sections through the canopy for all conditions investigated. The average static-pressure coefficients measured along the inner surface of the canopy are also shown on the respective figures for each test condition. These internal pressure coefficients are averages obtained from measurements made at six points on the inner surface located as shown in figure 4. Average internal pressure coefficients are shown inasmuch as the coefficients were uniform at the six points of measurement for all configurations investigated. The variation of internal static-pressure coefficient with yaw is shown in figure 14 for the complete range of airplane attitudes tested with canopy closed and propeller operating.

External Pressure Distributions

Zero yaw.- The results of the tests made with the airplane at zero yaw attitude both with propeller removed and with propeller operating are presented in figures 6 and 7. With the propeller removed (fig. 6), the results show that the lateral pressure coefficient distributions

are essentially symmetrical at all stations for the complete range of test conditions. For the low lift coefficient range (figs. 6(a) and 6(b)) peak negative pressure coefficients of approximately -0.70 exist on the front 3 lateral stations and diminish progressively for the more rearward stations, becoming slightly positive at the last station of measurement (station 6). For the high lift-coefficient range (figs. 6(c) and 6(d)), the characteristics of the pressure distributions are essentially unchanged although the magnitude of the peak negative pressure coefficients increases gradually with increasing lift coefficient, reaching peak values as high as -0.95 at the top of the front sections as shown in figure 6(d).

With propeller operating (fig. 7), the pressure coefficients are appreciably higher due to the increased local velocity in the propeller slipstream, and the lateral distribution of pressure on the canopy becomes quite asymmetrical at the higher thrust condition due to slipstream rotation. The results indicate that due to this pressure asymmetry, side loads exist tending to force the front of the canopy toward the right and the rear toward the left. As shown by the figures, opening the canopy results in more pronounced pressure asymmetry at the front stations of the canopy but causes a definite reduction in the magnitude of the external pressure coefficients. Based on the external-internal pressure differential and approximate flight dynamic pressures corresponding to the respective lift coefficients, these results indicate that the total net exploding load on the canopy will be greatest when the airplane is operating at high speed with canopy closed. However, as the results show that increasing lift coefficient causes a slight increase in the external pressure coefficient, a slightly greater load should be anticipated for a high-speed pull out than for the high-speed level flight condition. It should also be noted that while local crushing loads are indicated for some conditions they appear to be small in comparison to the critical exploding loads.

Negative yaw.- Figures 8 and 9 present the results of tests made with propeller removed and the airplane at negative yaw attitudes (right wing advanced) of -7.5 and -15 degrees. The effect of negative yaw as indicated by these results is to produce asymmetry in the pressure distributions. The asymmetry is most pronounced at the front sections of the canopy where the greatest negative pressure coefficients occur on the side toward the retarded wing, whereas for the three rear stations the asymmetry is less pronounced with highest negative pressures on the side toward the advancing wing.

As compared to propeller-removed results at zero yaw (fig. 6) it is seen that in addition to the pressure asymmetry produced by yaw, the magnitude of the peak negative pressure for a given lift coefficient

is also increased as the yaw angle increases. With propeller operating (figs. 10 and 11) the results show that the pressure asymmetry is reduced inasmuch as the slipstream rotation tends to oppose the angle of flow over the canopy induced by negative yaw. As previously noted at zero yaw the magnitude of the pressure coefficients are appreciably increased at the higher thrust coefficients due to the increased slipstream velocity over the canopy. Throughout the range of negative yaw angles, opening the canopy increases the asymmetry of distribution at the front canopy stations but causes a general reduction in the magnitude of the pressure coefficients over the complete canopy. The results indicate that the canopy net loads will be most critical with canopy closed through the negative yaw range inasmuch as the differential external-internal pressure coefficient decreases rapidly when the canopy is opened.

Positive yaw.- The results of the tests made at positive yaw attitudes (right wing retarded) with the propeller operating are presented in figures 12 and 13. From these figures it is seen that at positive yaw attitudes the asymmetry of flow over the canopy due to yaw combines with the flow asymmetry and increased local velocities of the propeller slipstream so that for any given lift coefficient the lateral asymmetry of pressure becomes very pronounced and the magnitude of the peak negative pressure coefficients increase appreciably as positive yaw is increased.

These results therefore indicate that the canopy loads encountered at positive yaw attitude will be much more extreme than the loads indicated for corresponding attitudes (same C_L and T_c) at either zero or negative yaw. As previously noted for zero and negative yaw attitudes, opening the canopy has the general effect of decreasing the external pressure coefficients although the asymmetry of pressure distribution becomes more pronounced at the front sections. Based on the differential external-internal pressure coefficients the results indicate that the greatest net loads will exist at all attitudes with canopy completely closed.

Internal Static Pressures

Static pressure coefficients measured at the inner surface of the canopy are shown in conjunction with the external pressure distributions presented in figures 6 to 13 for the complete range of test conditions. In addition, figure 14 is presented to summarize the variation of internal pressure coefficient with yaw angle for the range of airplane attitudes investigated with the canopy closed and propeller operating. As shown by the results the highest internal negative pressure coefficients occur when the canopy is open 3 inches and the least negative pressure coefficients occur with canopy closed.

For the zero yaw attitude with propeller operating, the internal pressure coefficients with canopy closed varied from 0 for $C_L = 1.18$ to −0.07 for $C_L = 0.10$ whereas with the canopy open 3 inches the pressure coefficients ranged from −1.02 to −0.54 for the same lift coefficients of 1.18 and 0.10, respectively. From figure 14 it is seen that for the canopy-closed condition the internal pressure coefficients remained approximately constant throughout the range of negative yaw attitudes but became increasingly negative as yaw increased through the positive range.

CONCLUDING REMARKS

The results of the investigation of pressure distributions on the bubble type single place canopy which was typified by the installation on the Grumman F9F-1 airplane show that:

1. The net exploding forces on the canopy will be greatest when the airplane is operating at high speed with canopy closed.

2. For all conditions the net canopy load will be in an exploding direction.

3. At all attitudes investigated, partially opening the canopy reduces the external negative pressure coefficients and increases the internal negative pressure coefficients thus reducing the net exploding loads.

4. Yawing the airplane increases the magnitude of the peak negative pressure coefficients and results in an asymmetrical lateral distribution of pressure which becomes more pronounced with increasing yaw.

5. The high axial velocities and rotation of the slipstream at high thrust conditions also increase the magnitude of the pressure coefficients and produce asymmetry in the distribution of pressure. The effects of propeller operation are most pronounced at positive yaw attitudes as the flow asymmetry due to clockwise slipstream rotation combines with the flow asymmetry due to positive yaw.

6. Increasing the lift coefficient causes a slight increase in the magnitude of the external pressure coefficients.

Langley Memorial Aeronautical Laboratory
National Advisory Committee for Aeronautics
Langley Field, Va.

REFERENCES

1. Cocke, Bennie W., Jr., and Czarnecki, K. R.: Canopy Loads Investigation for the F6F-3 Airplane. NACA RM No. L6L23a, 1946.

2. Dexter, Howard E., and Rickey, Edward: Investigation of the Loads on a Conventional Front and Rear Sliding Canopy. NACA RM No. L7D04, 1947.

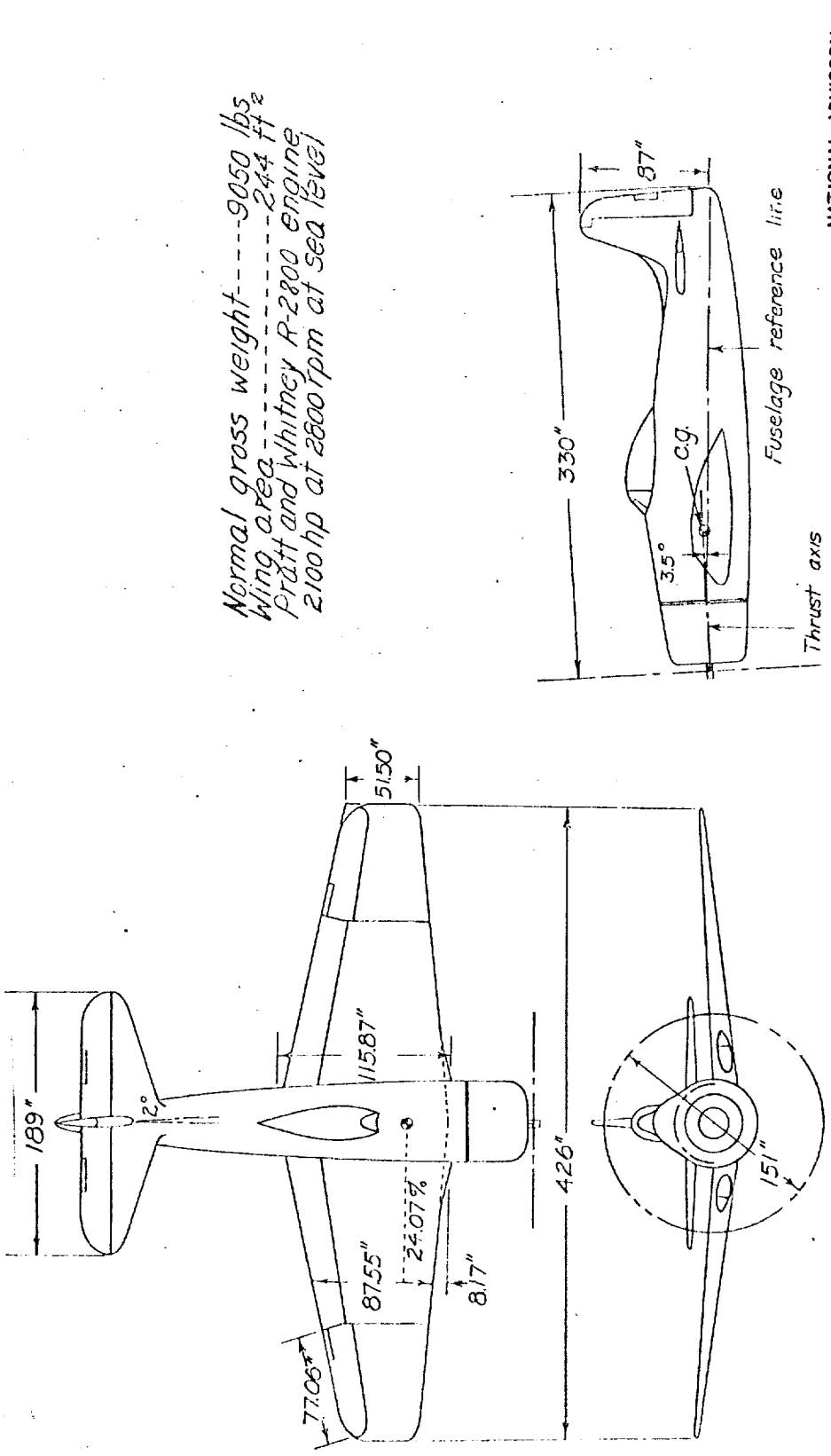

Figure 1 - Three-view drawing of the XF8F-1 airplane.

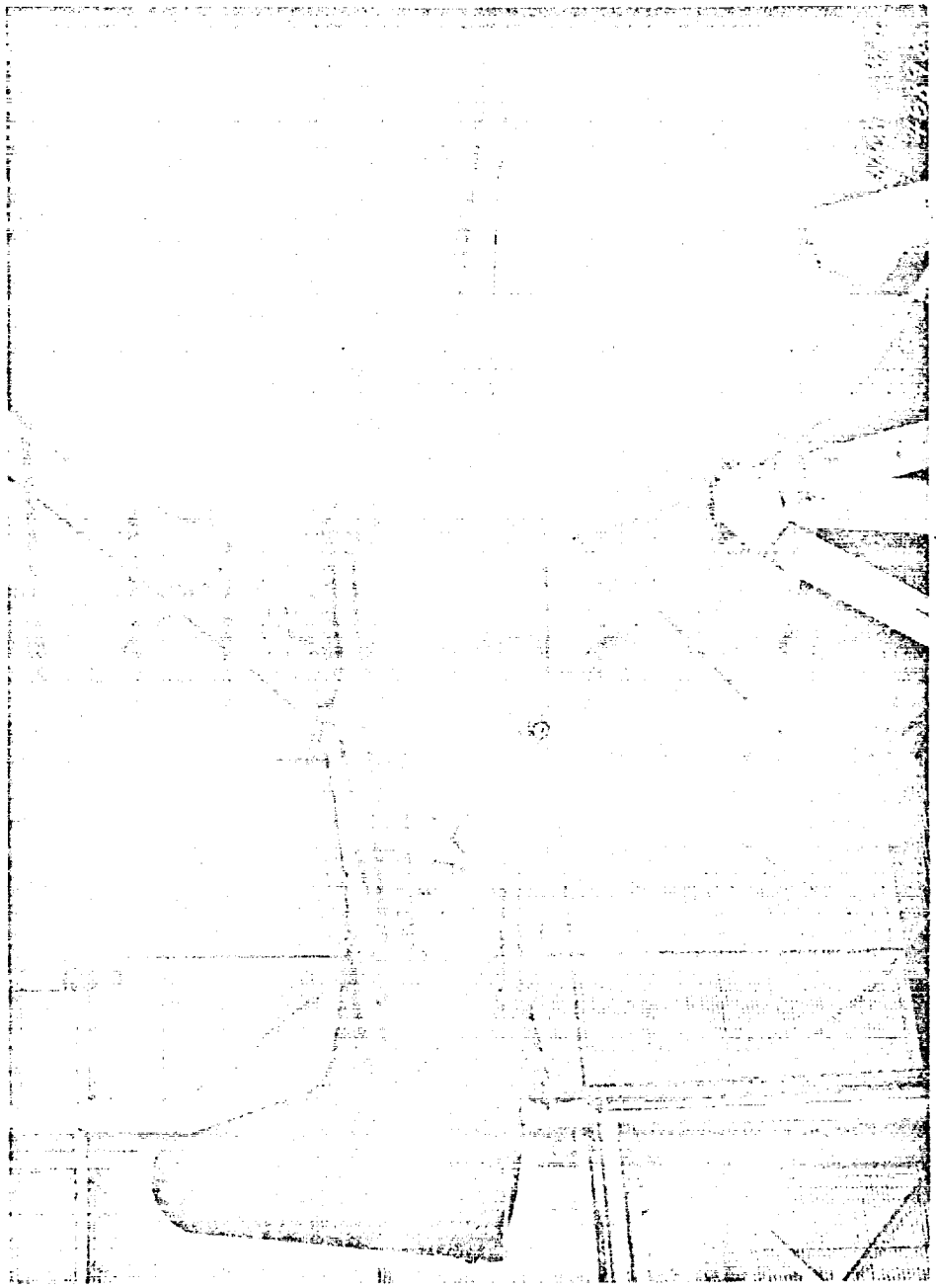

Figure 2.- The F8F-1 airplane mounted in the Langley full-scale tunnel.

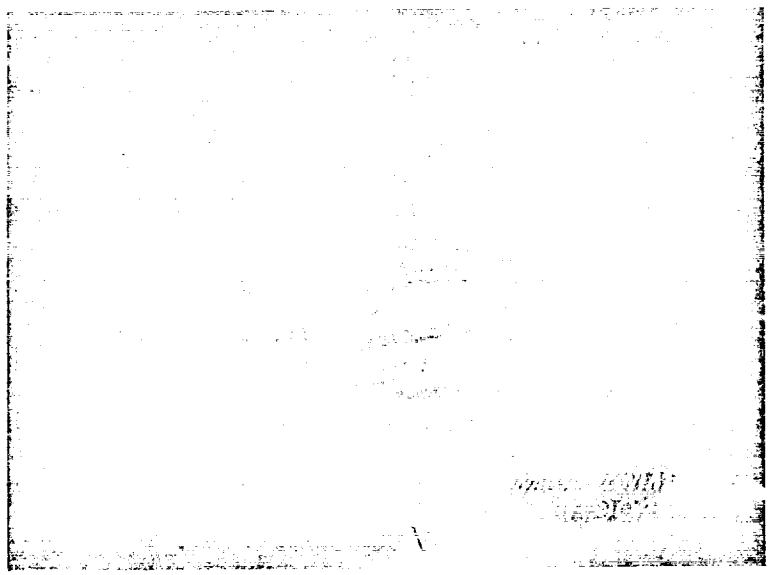

(a) Canopy closed.

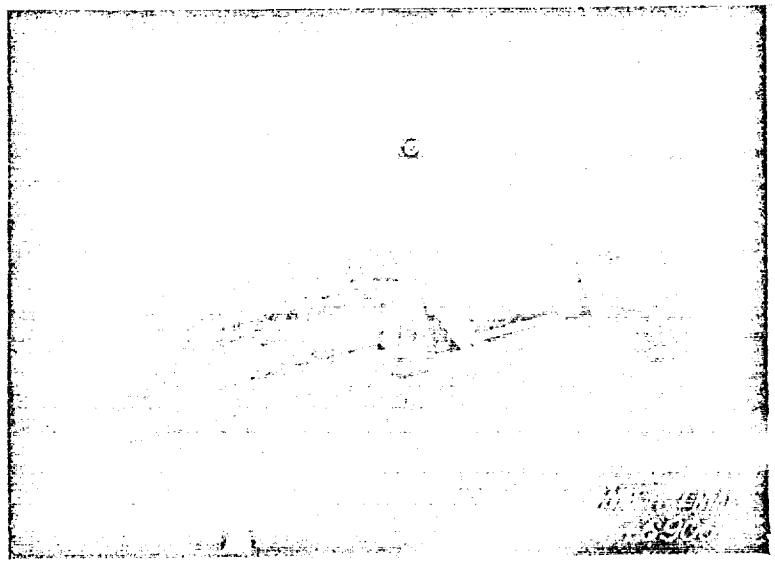

(b) Canopy full open.

Figure 3.- Photographs showing the general arrangement of the bubble-type canopy on the F8F-1 airplane.

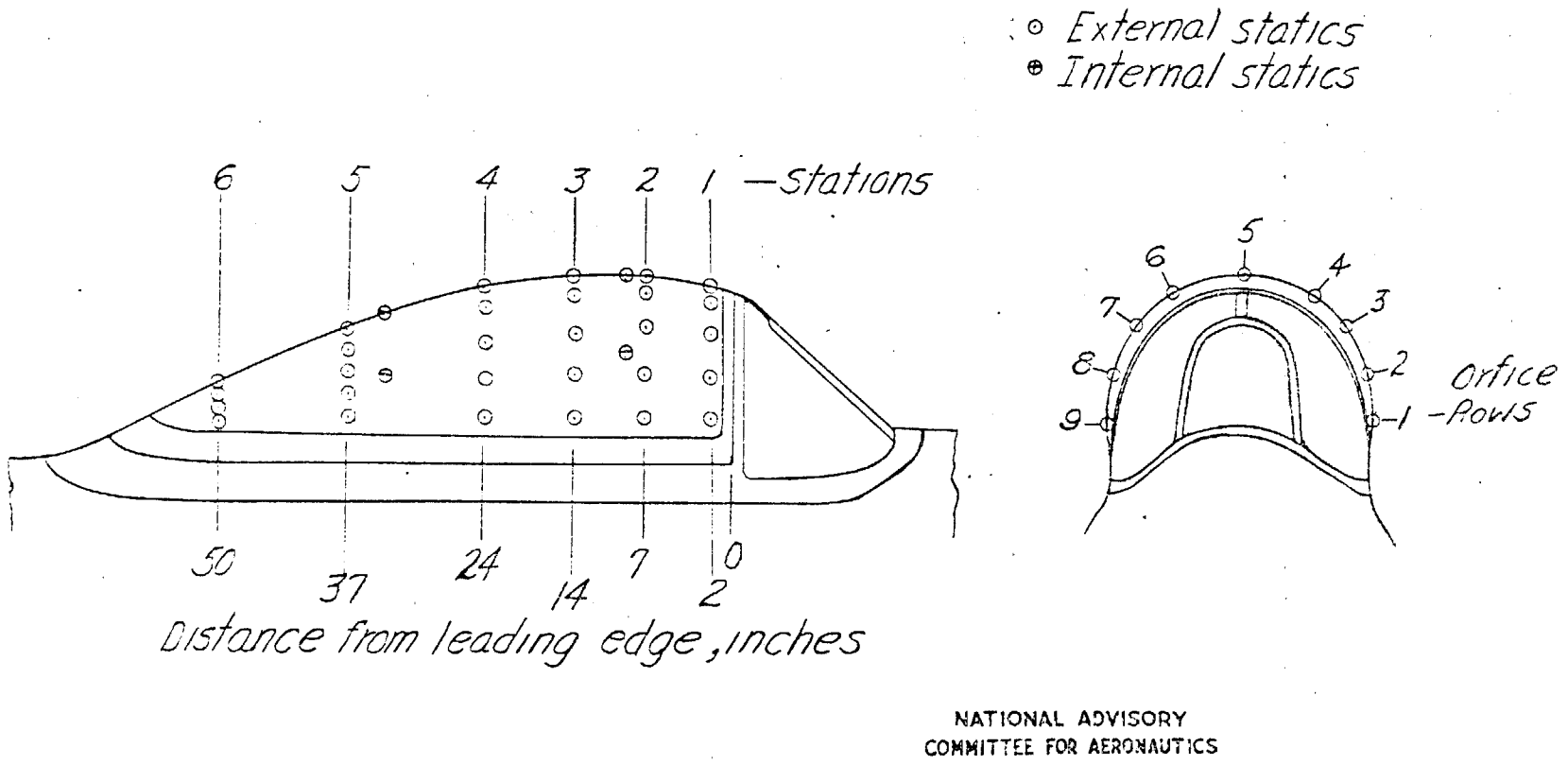

Figure 4.- Pressure measurement station locations for the F8F-1 canopy.

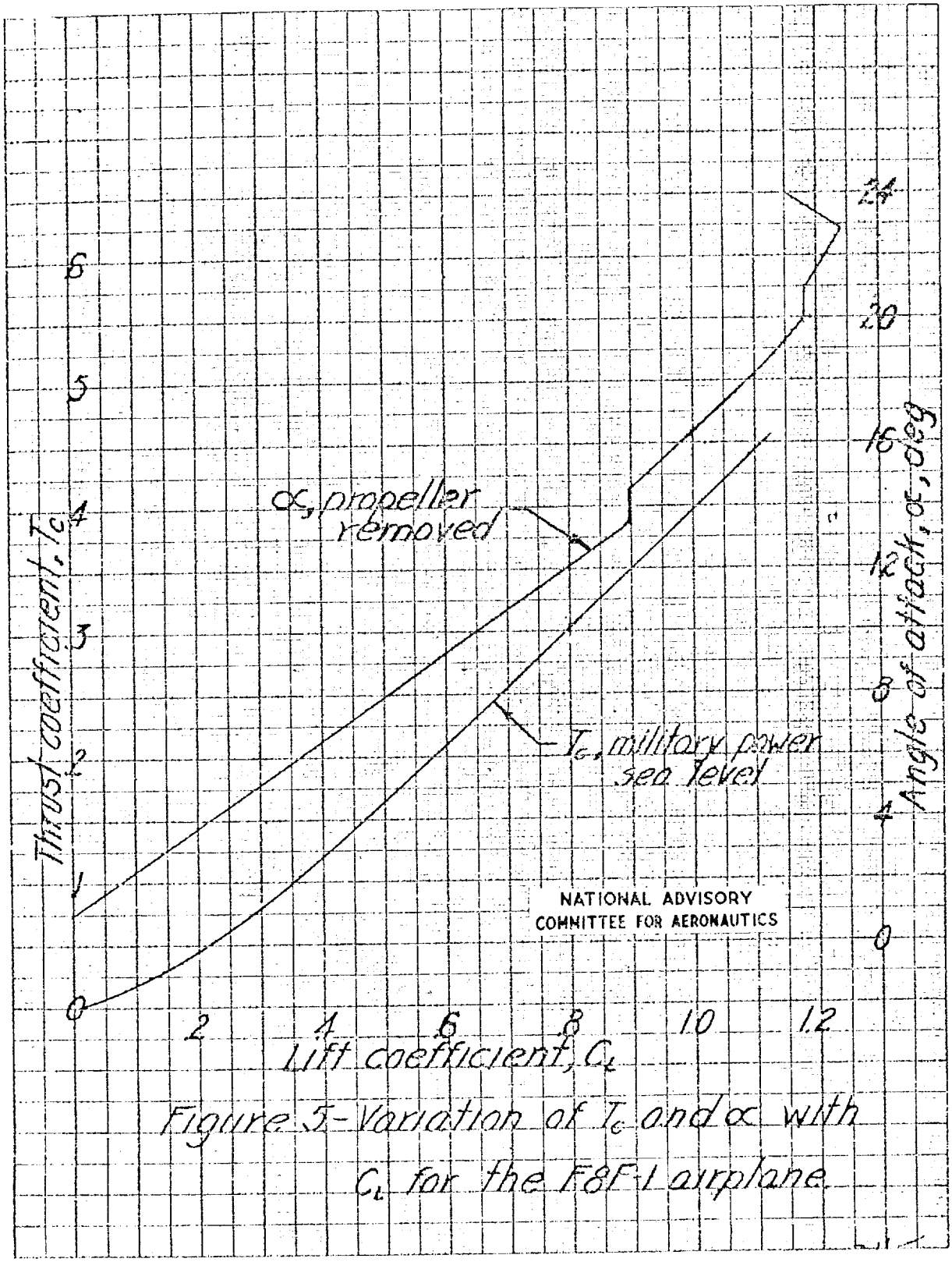

Figure 5- Variation of T_c and α with C_L for the F8F-1 airplane.

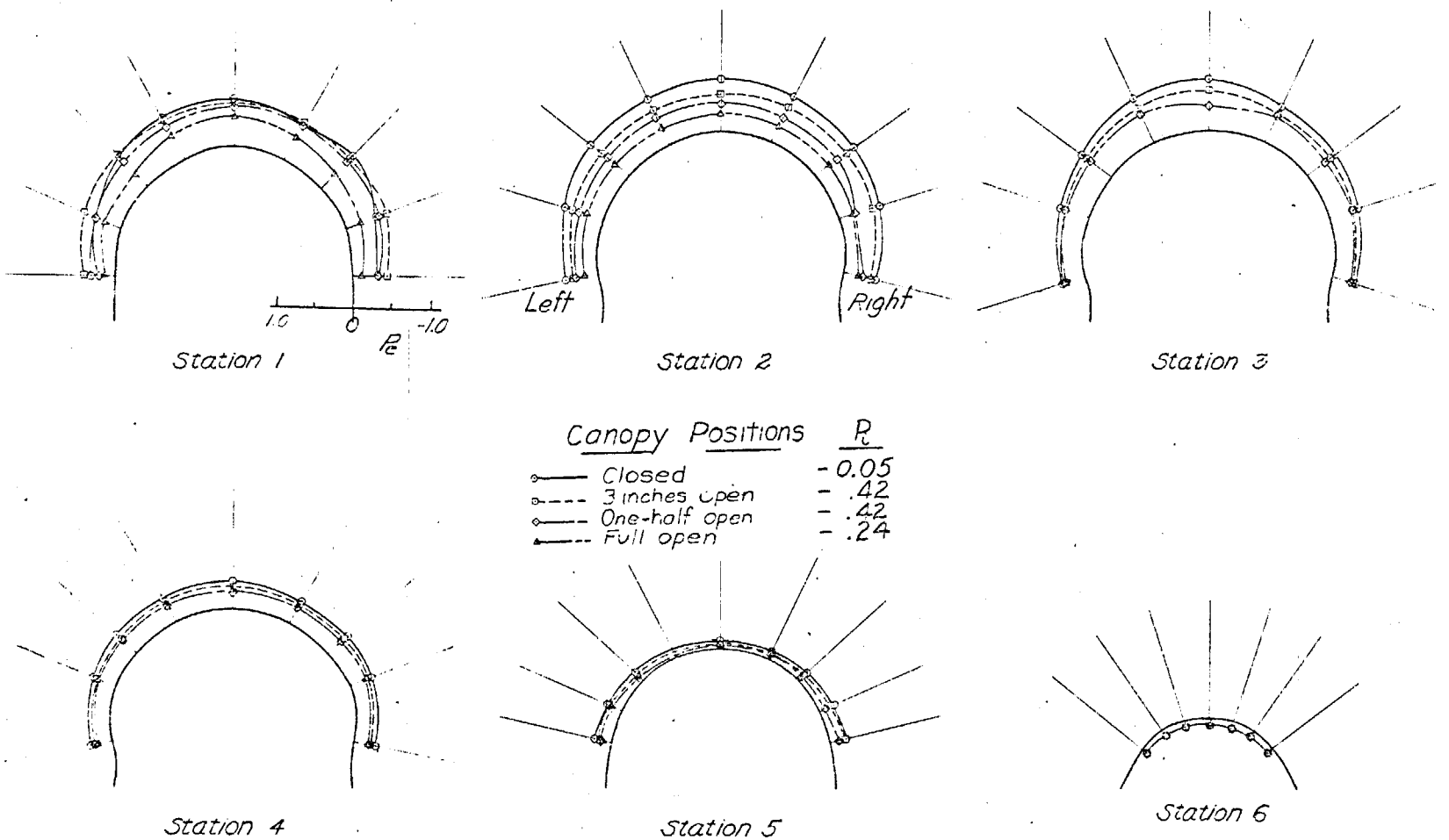

(a) Propeller removed; C_L, 0.10

Figure 6.—Pressure distributions over the canopy of the F8F-1 airplane. α, 0°

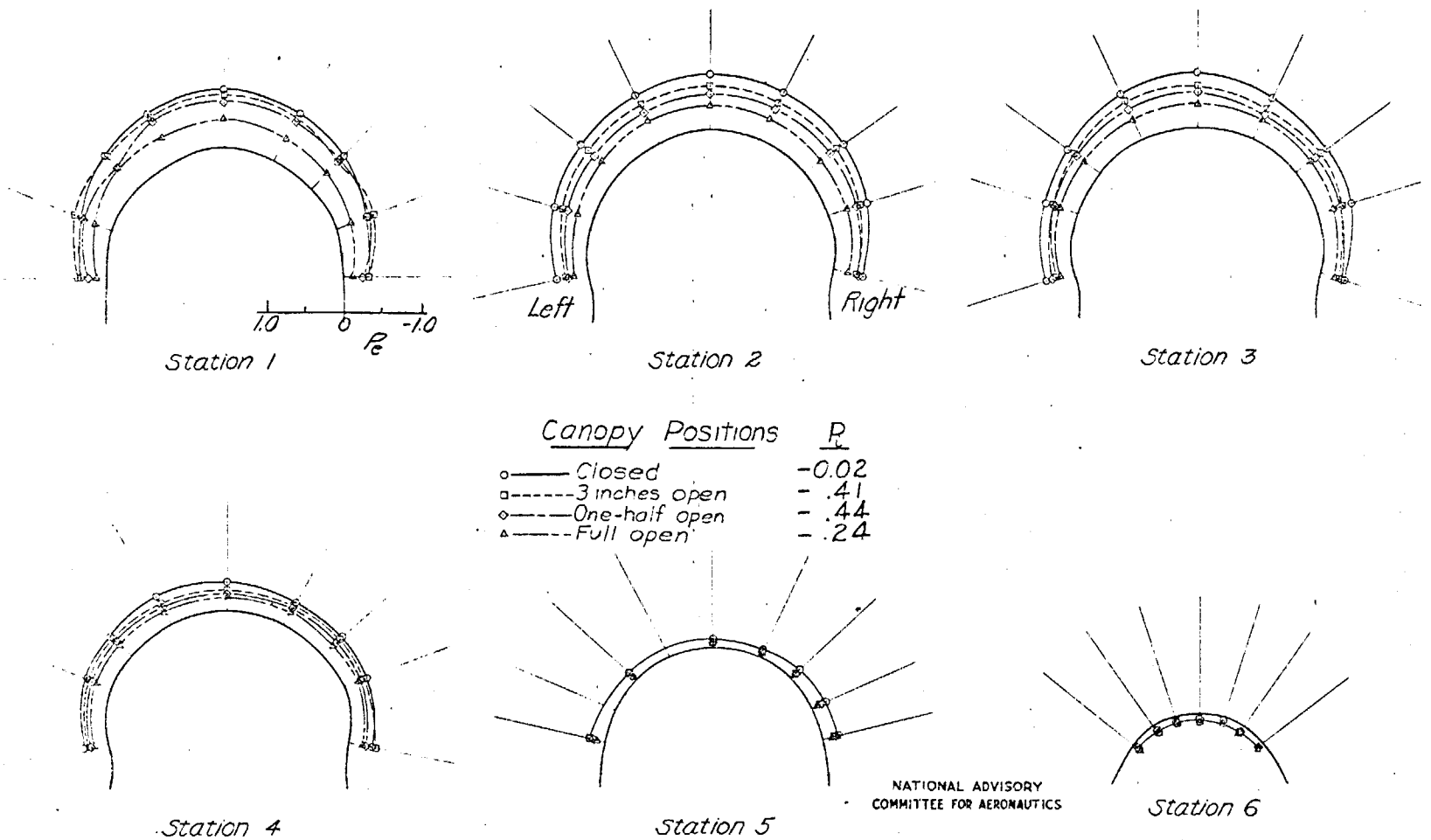

(b) Propeller removed; C_L, 0.50

Figure 6.– Continued.

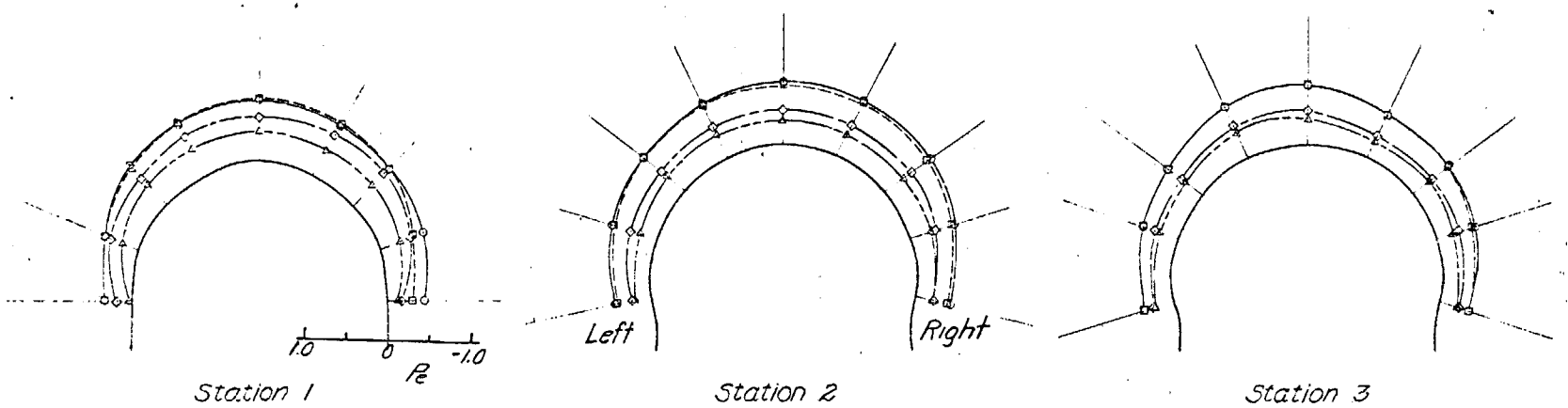

Station 1 Station 2 Station 3

Canopy Positions R_z

Closed	0.0
3 inches open	- .43
One-half open	- .44
Full open	- .24

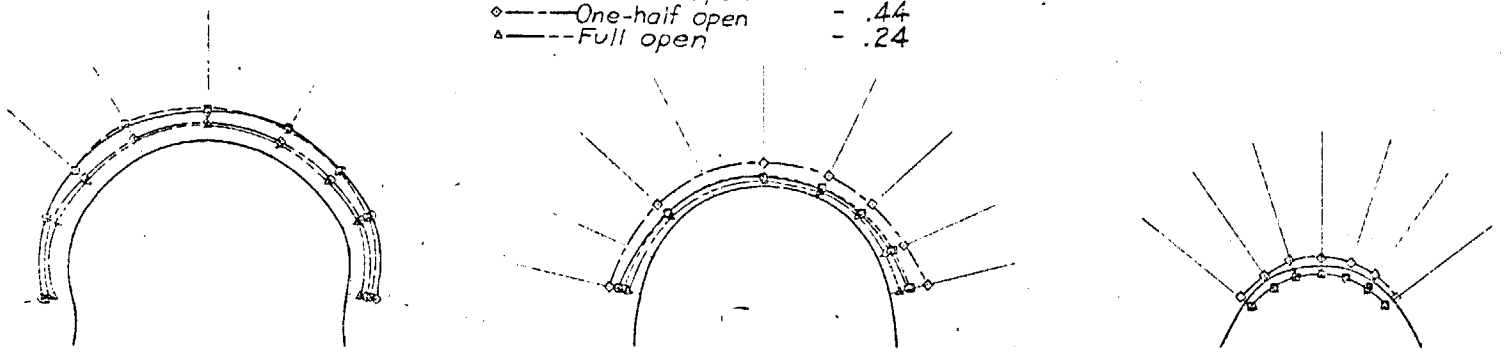

Station 4 Station 5 Station 6

NATIONAL ADVISORY COMMITTEE FOR AERONAUTICS

(c) Propeller removed; C_L, 0.87

Figure 6.- Continued.

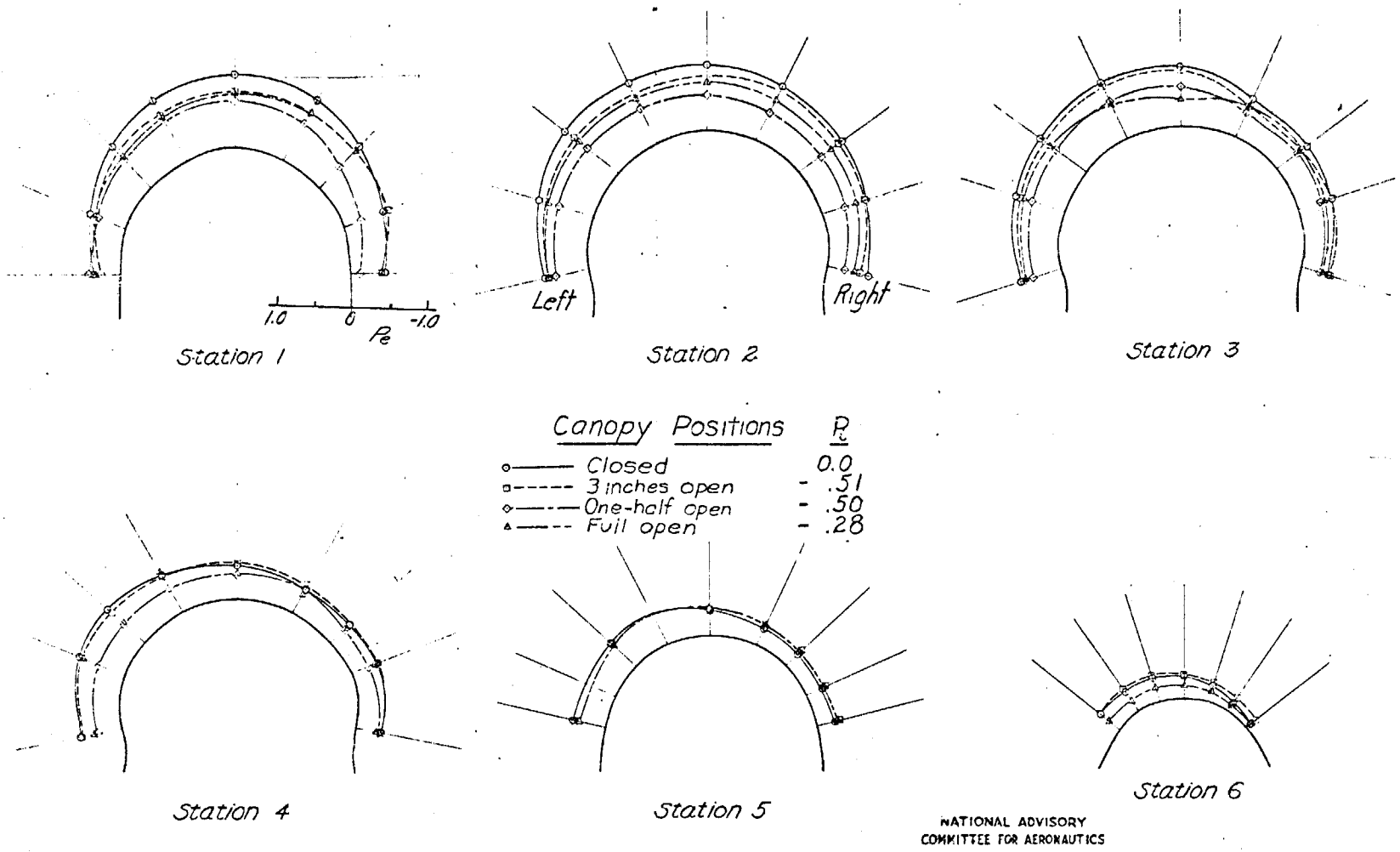

(d) Propeller removed; C_L, 1.18

Figure 6.- Concluded.

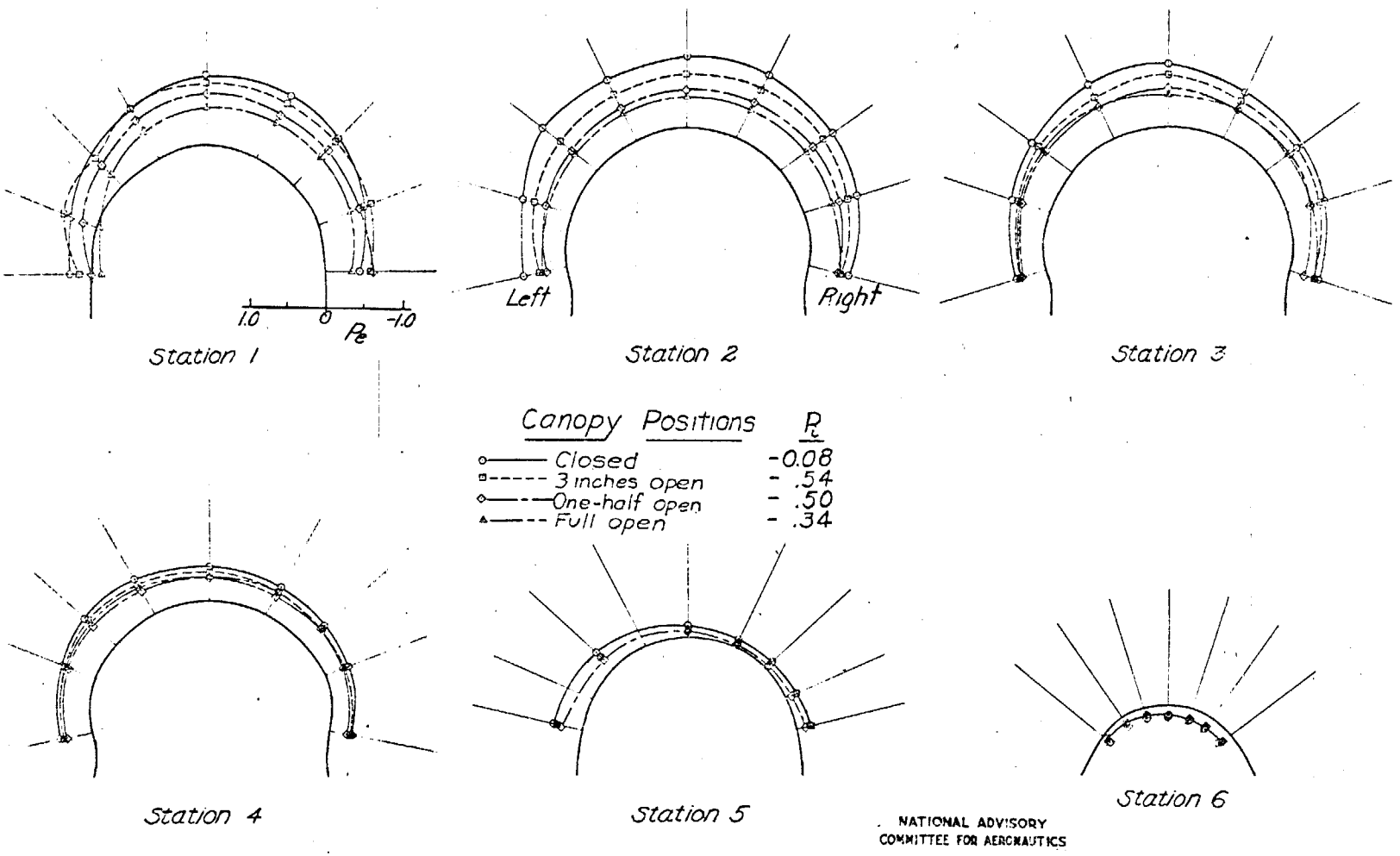

(a) Military power; T_c, 0.02; C_L, 0.10

Figure 7.- Pressure distributions over the canopy of the F8F-1 airplane. α, 0°

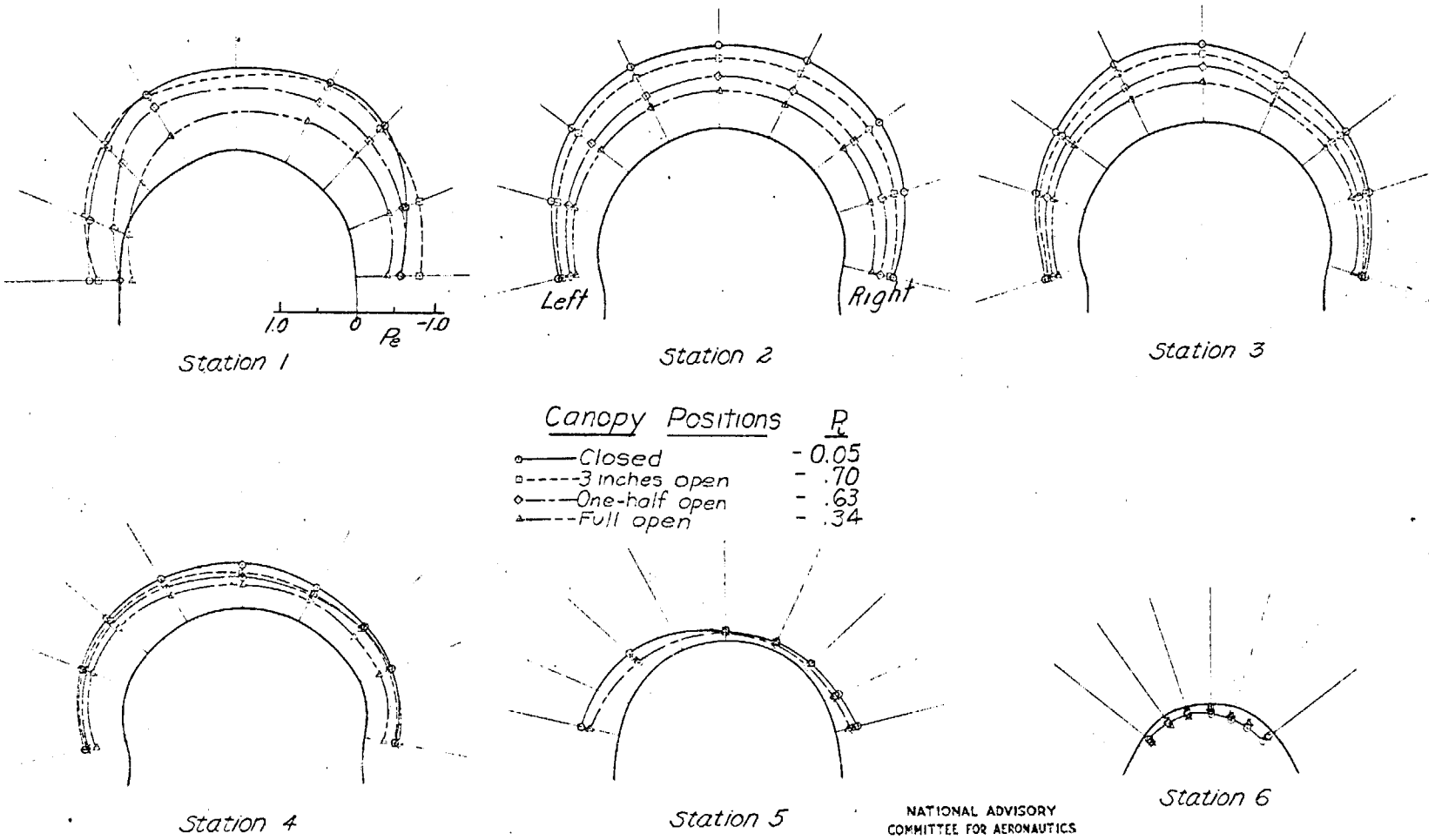

(b) Military power; T_c, 0.17; C_L, 0.50

Figure 7.- Continued.

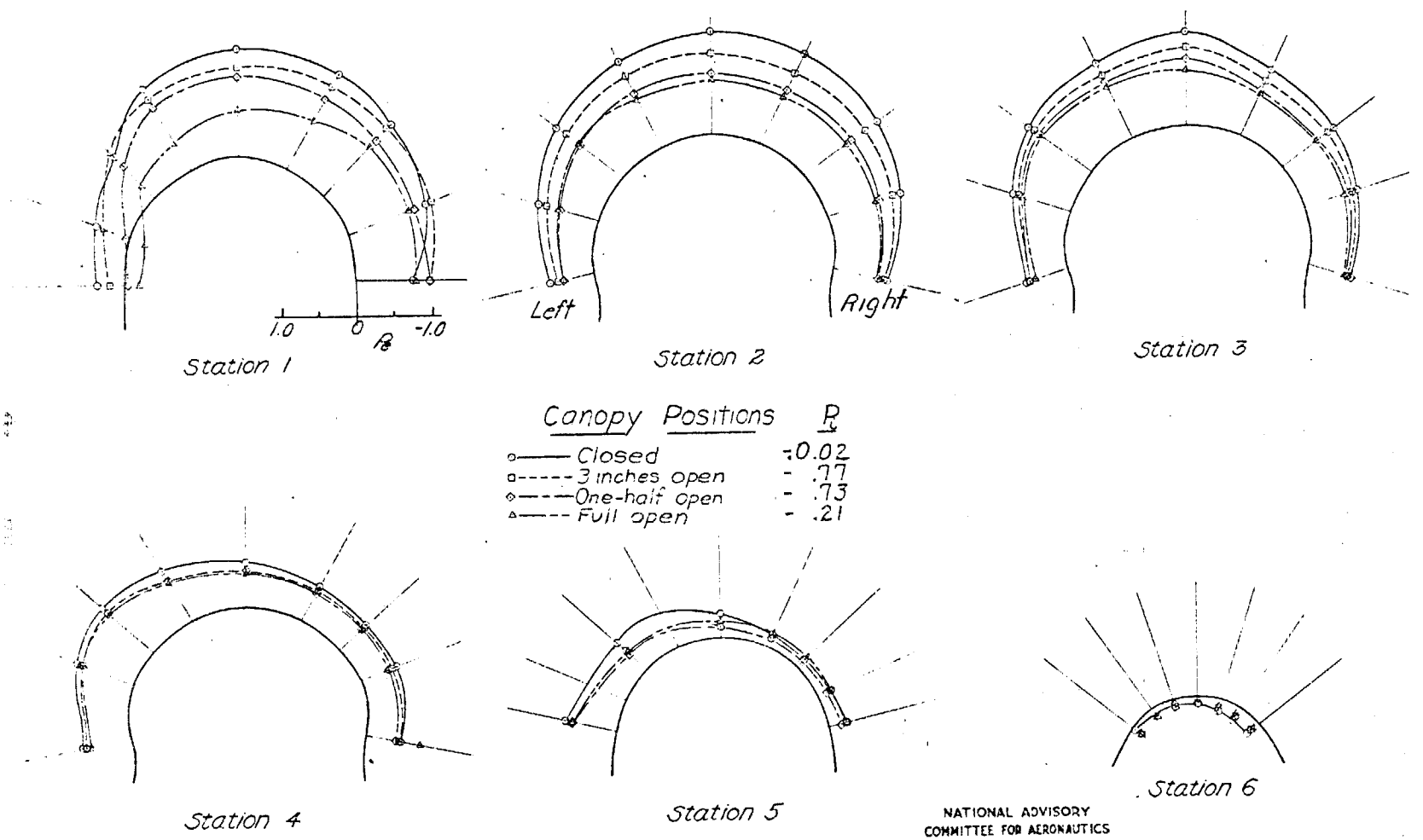

(c) Military power; T_c, 0.34; C_L, 0.87

Figure 7.- Continued.

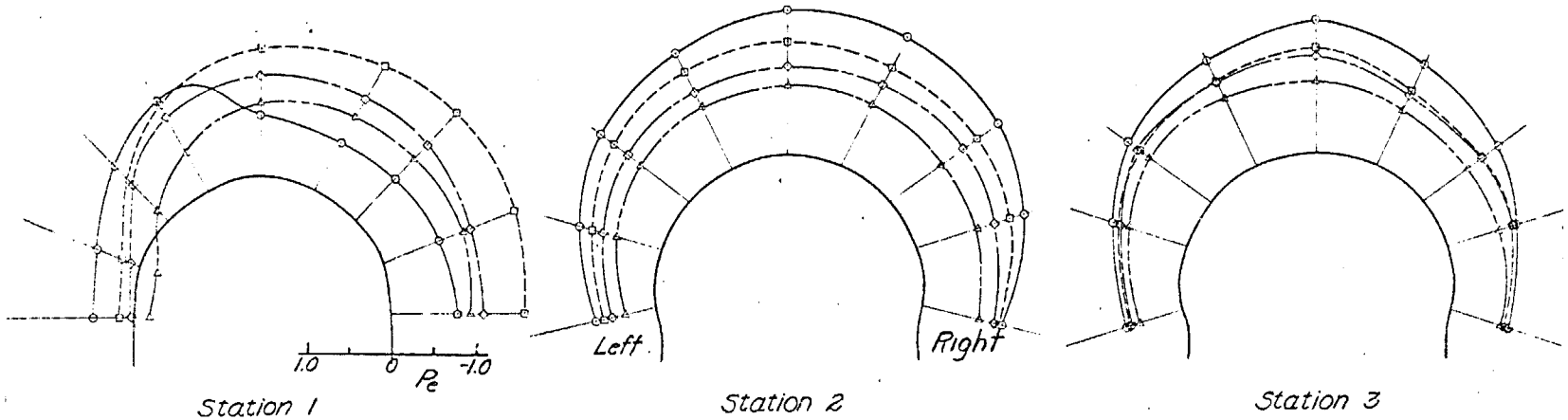

Station 1 Station 2 Station 3

Canopy Positions P_t

Closed	0.0
3 inches open	-1.02
One-half open	-0.83
Full open	- .38

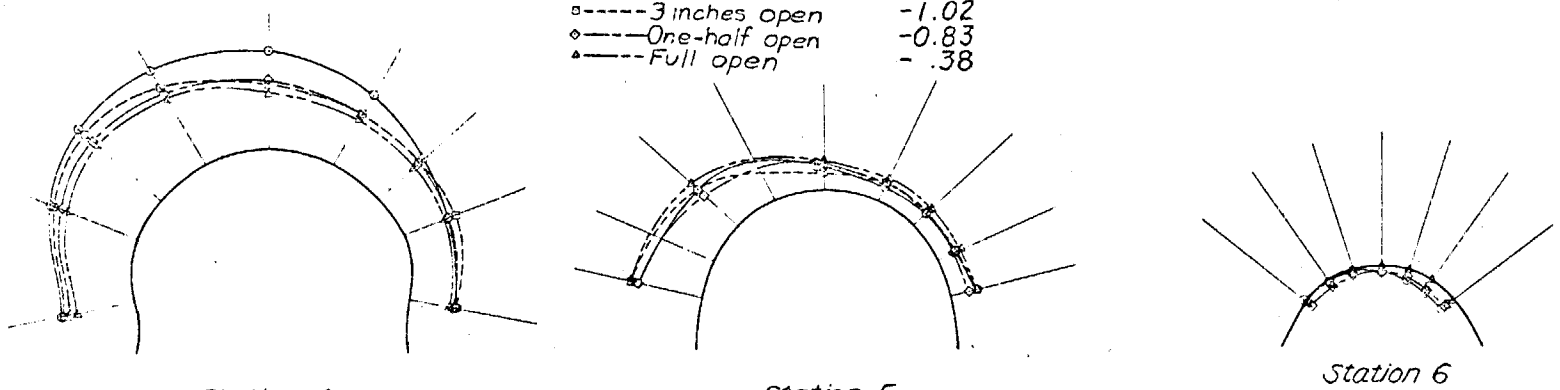

Station 4 Station 5 Station 6

NATIONAL ADVISORY COMMITTEE FOR AERONAUTICS

(d) Military power; T_c, 0.48; C_L, 1.18

Figure 7.—Continued

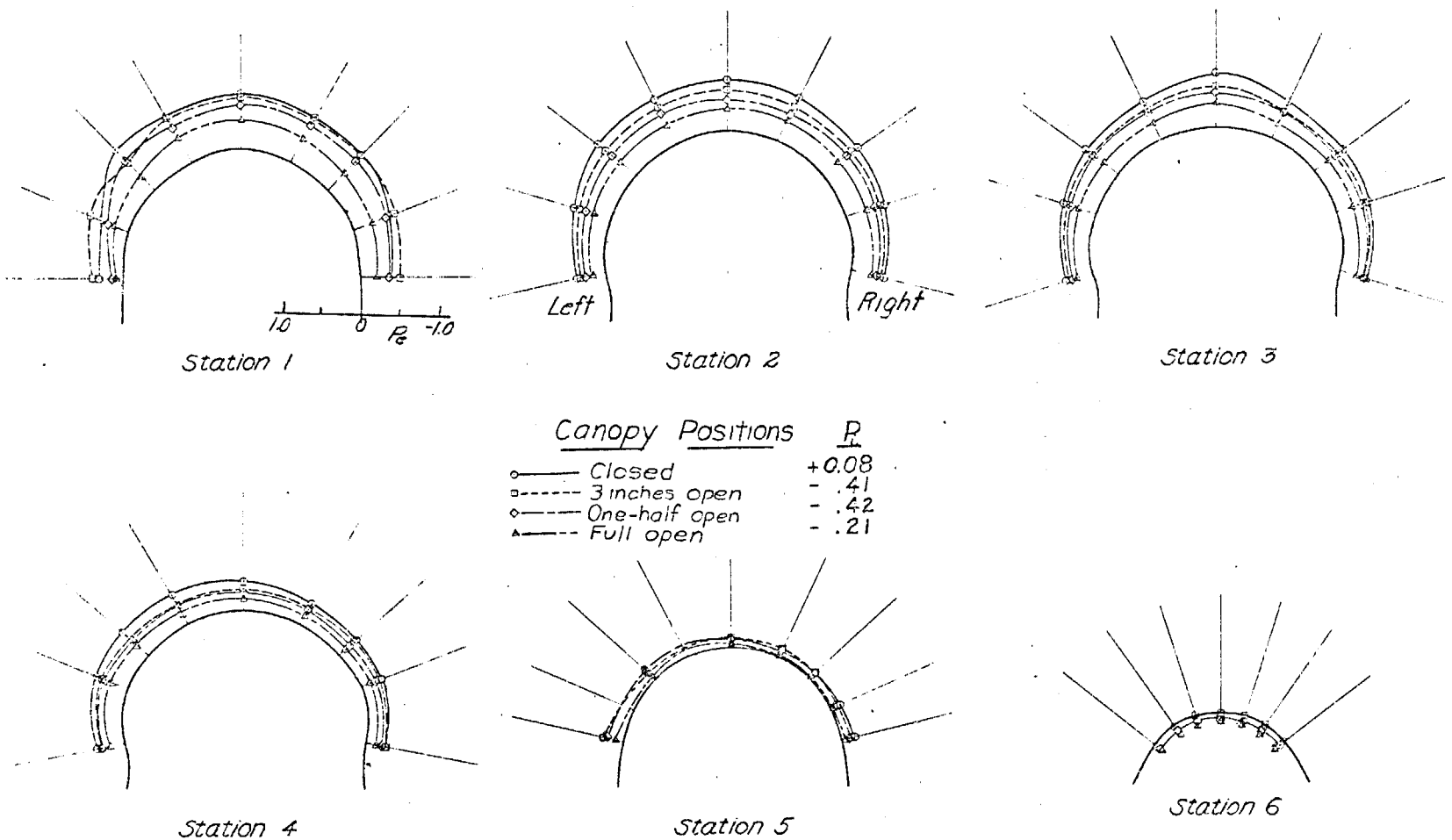

NATIONAL ADVISORY COMMITTEE FOR AERONAUTICS

(e) Propeller idling; C_L, 1.18

Figure 7.- Concluded.

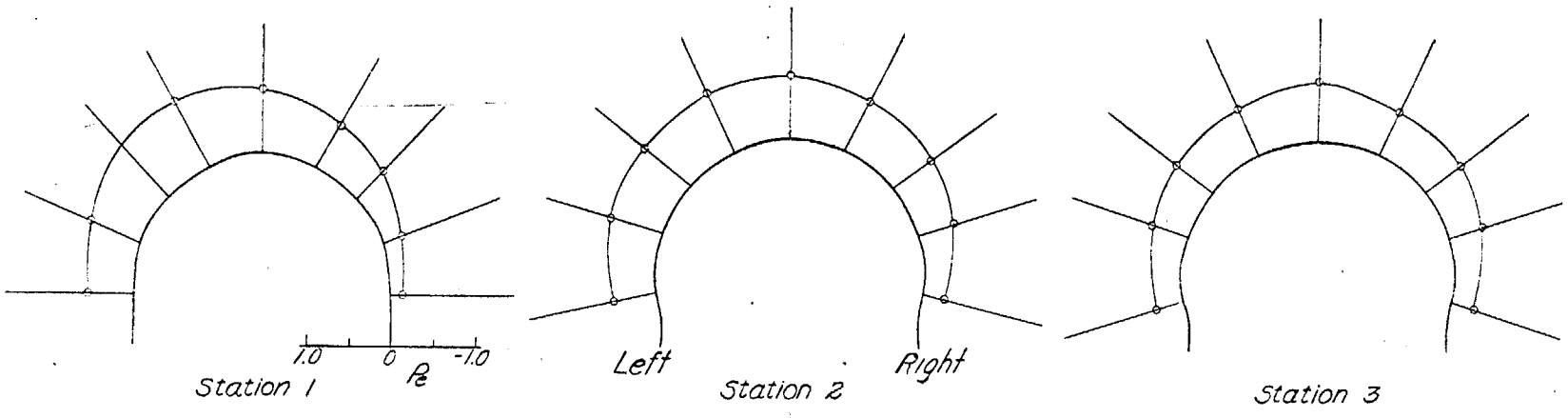

Canopy closed, $P_t = -0.09$

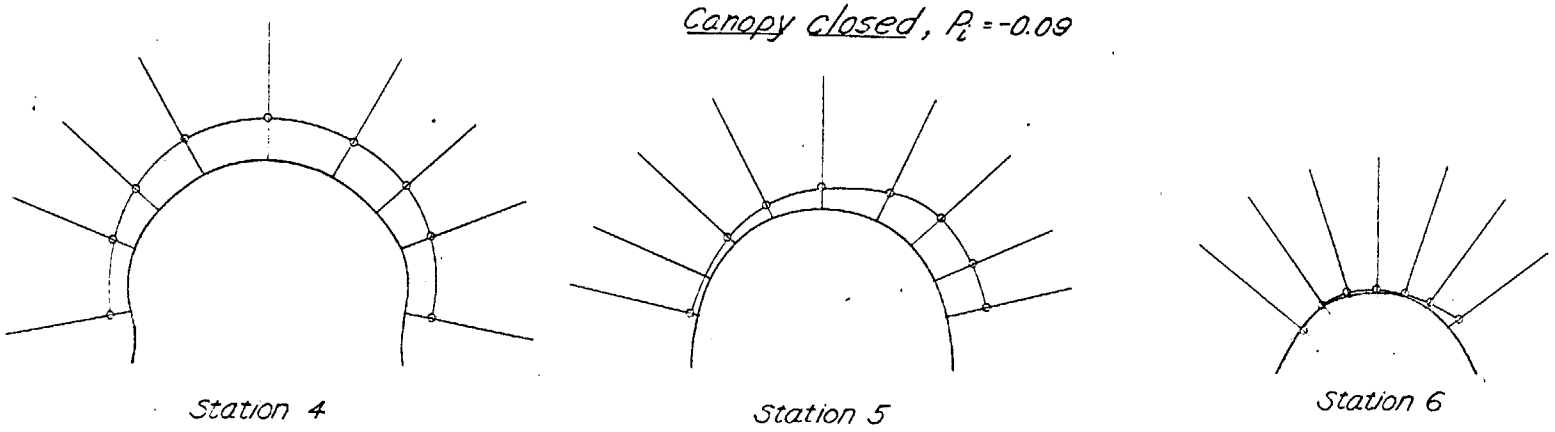

NATIONAL ADVISORY COMMITTEE FOR AERONAUTICS

(a) Propeller removed; C_L, 0.10

Figure 8.—Pressure distributions over the canopy of the F8F-1 airplane. α, -7.5°

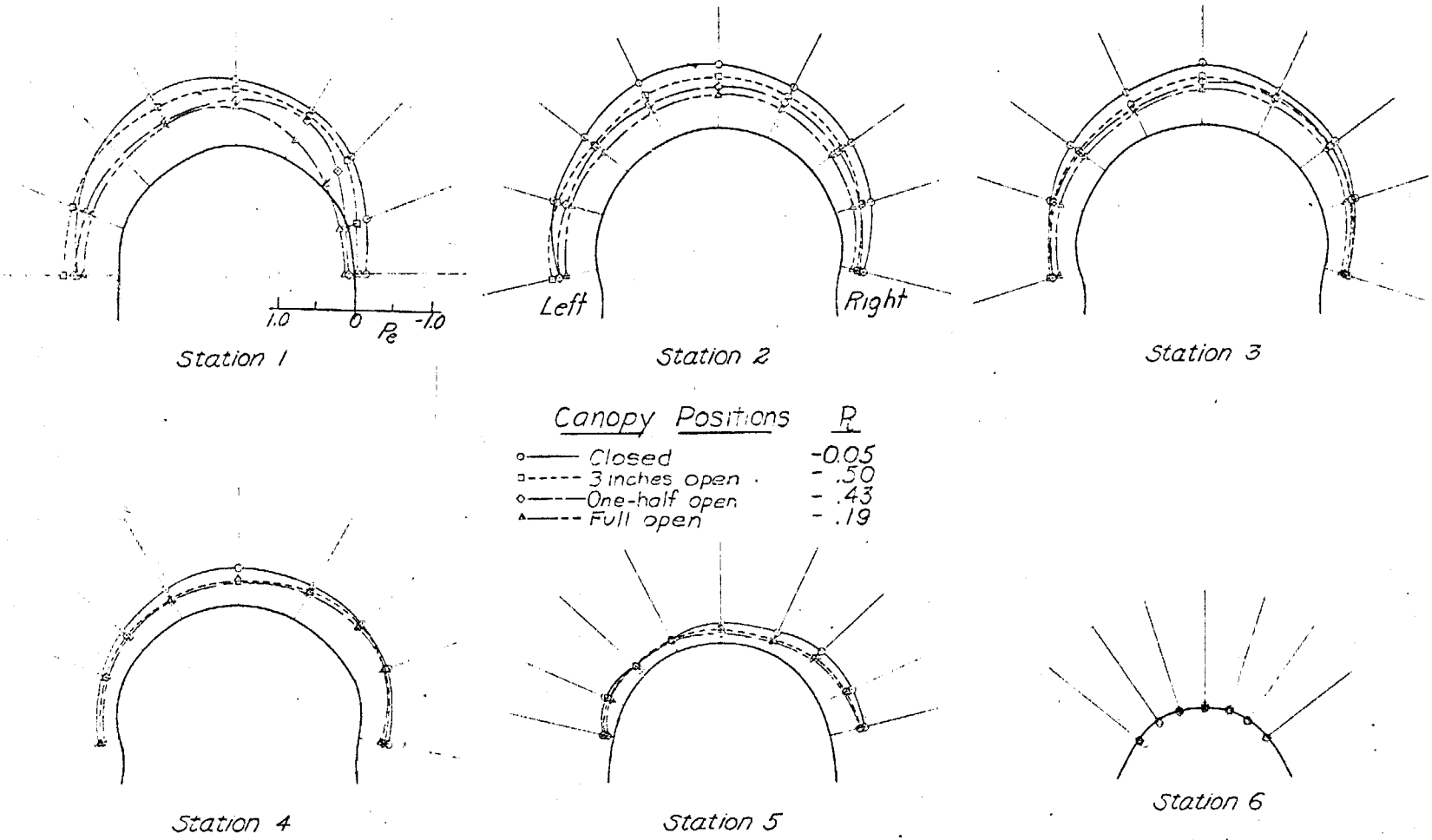

(b) Propeller removed; C_L, 0.50

Figure 8.- Continued

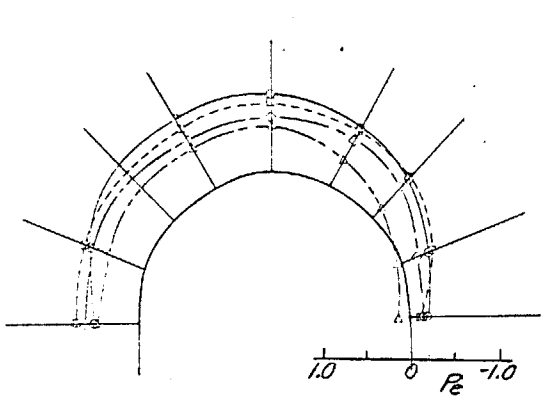

Station 1

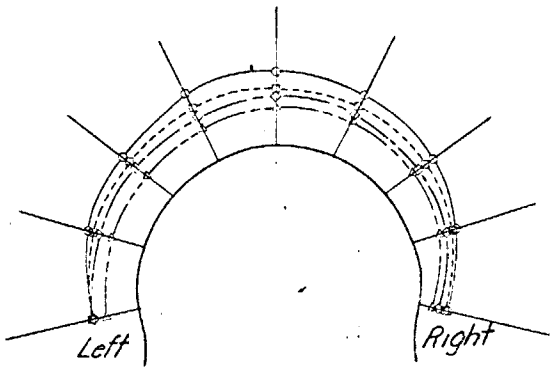

Station 2

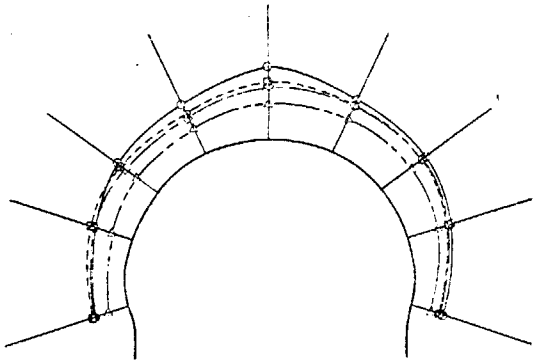

Station 3

Canopy Positions P_t

Closed	+0.04
3 inches open	- .50
One-half open	- .48
Full open	- .19

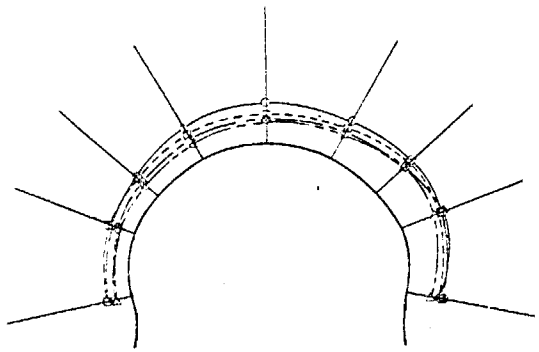

Station 4

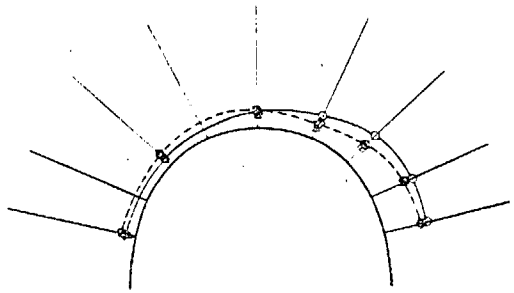

Station 5

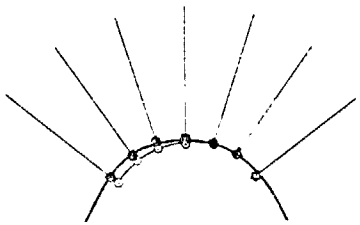

Station 6

(C) Propeller removed; C_L, 0.87

NATIONAL ADVISORY COMMITTEE FOR AERONAUTICS

Figure 8.-Continued.

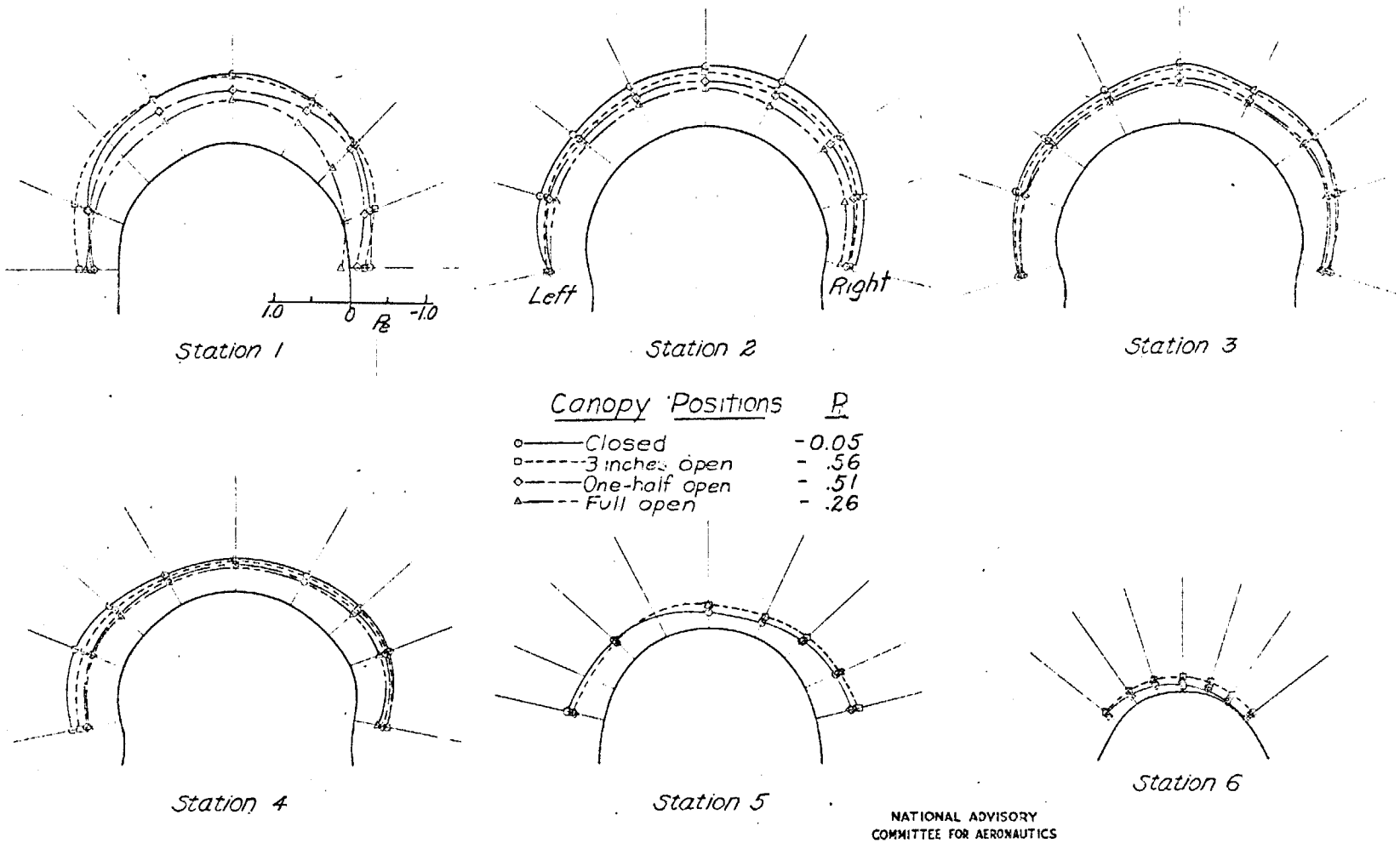

(d) Propeller removed; C_L, 1.18

Figure 8.- Concluded.

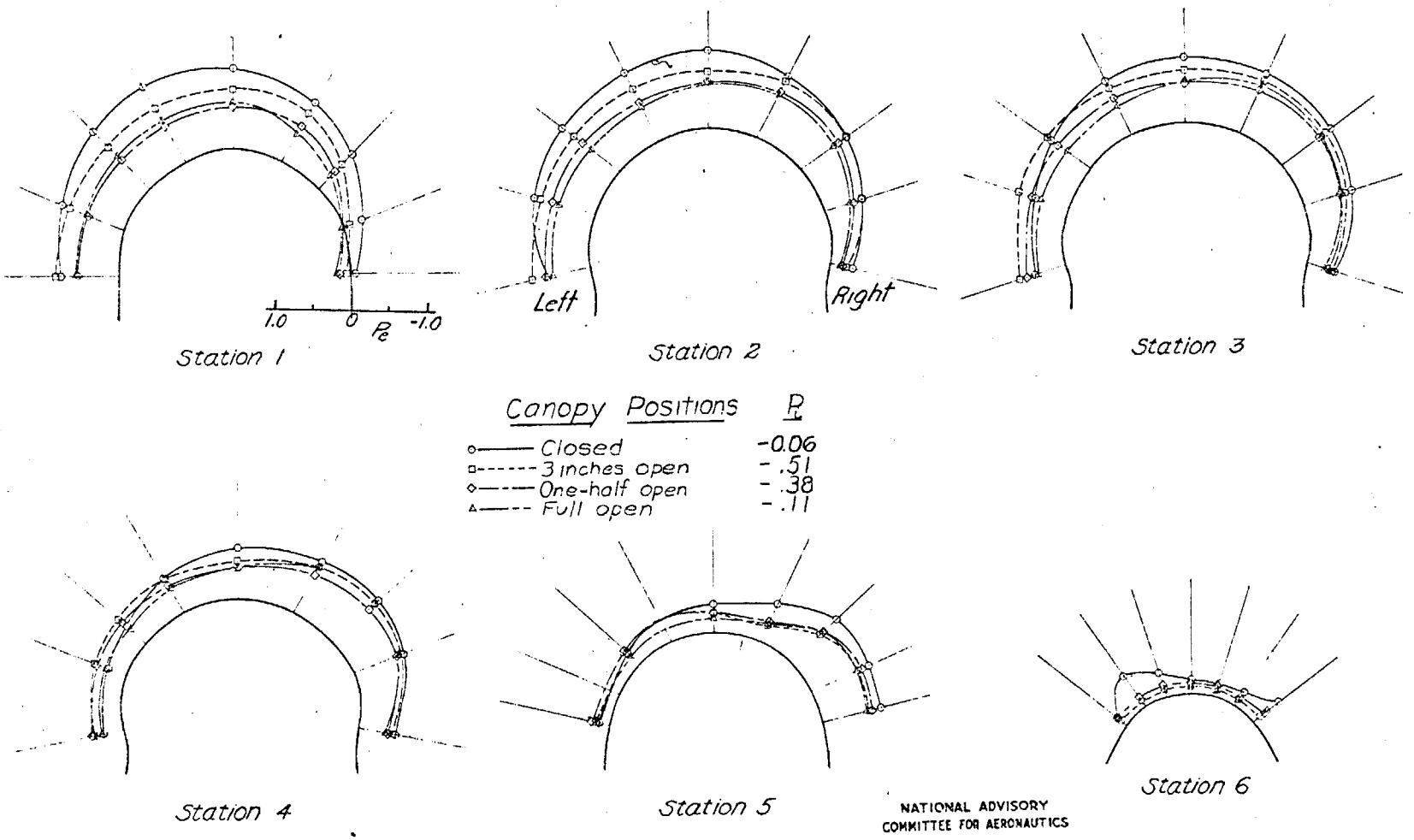

(a) Propeller removed; C_L, 0.87

Figure 9.- Pressure distributions over the canopy of the F8F-1 airplane. α, -15°

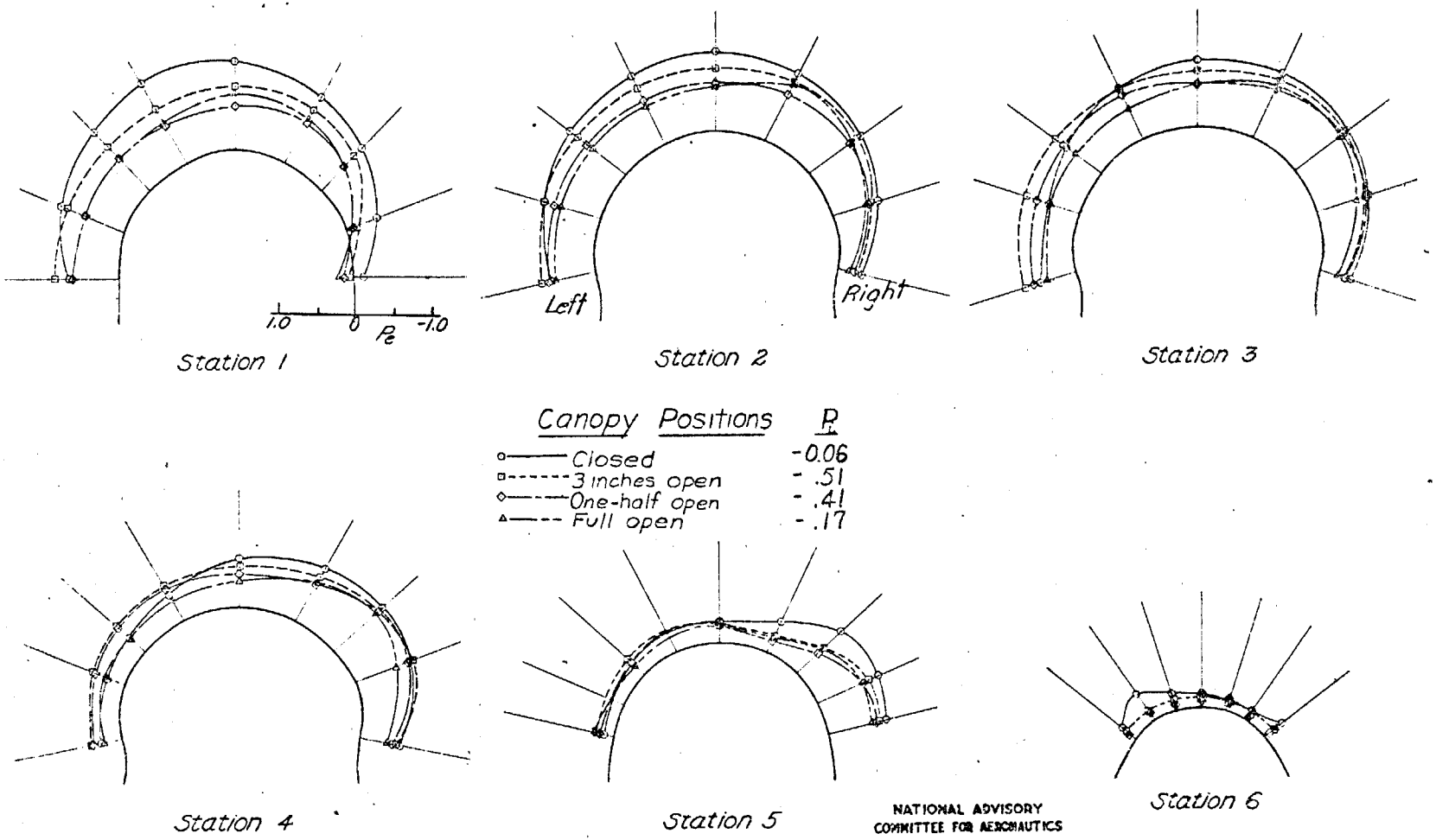

(b) Propeller removed; C_L, 1.18

Figure 9.- Concluded.

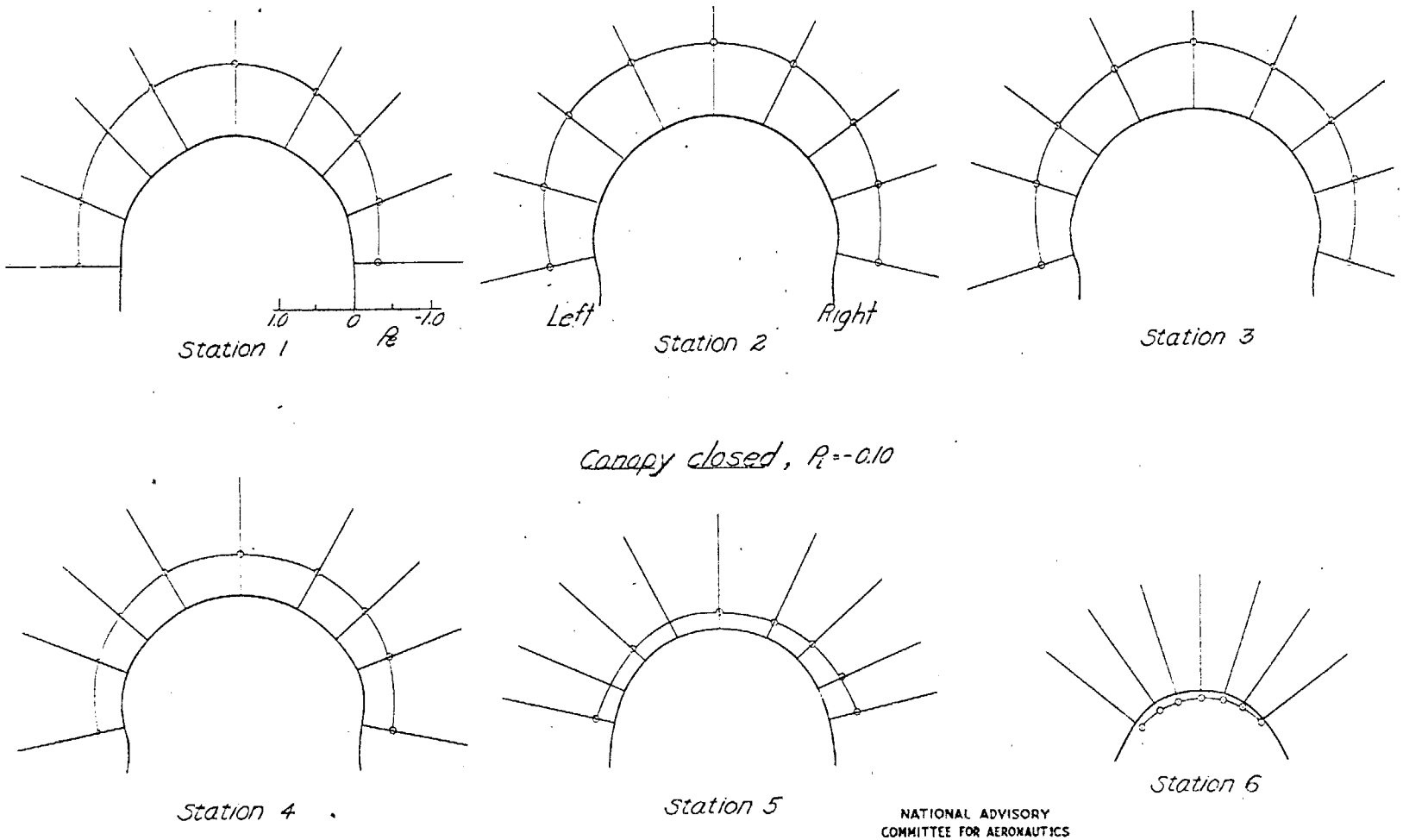

(a) Military power; T_c, 0.02; C_L, 0.10

Figure 10.-Pressure distributions over the canopy of the F8F-1 airplane. α, -7.5

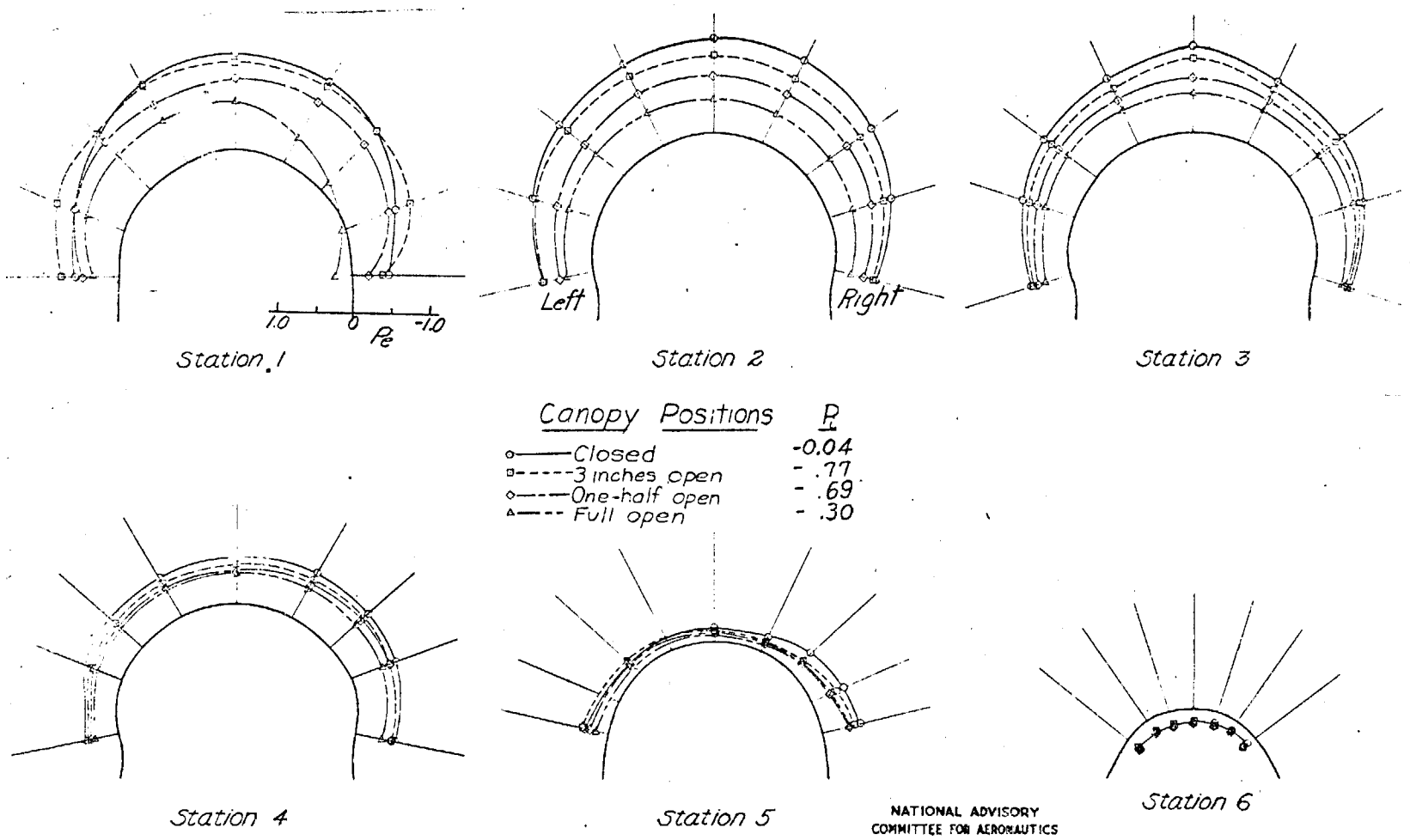

(b) Military power; T_c, 0.17; C_L, 0.50

Figure 10.-Continued.

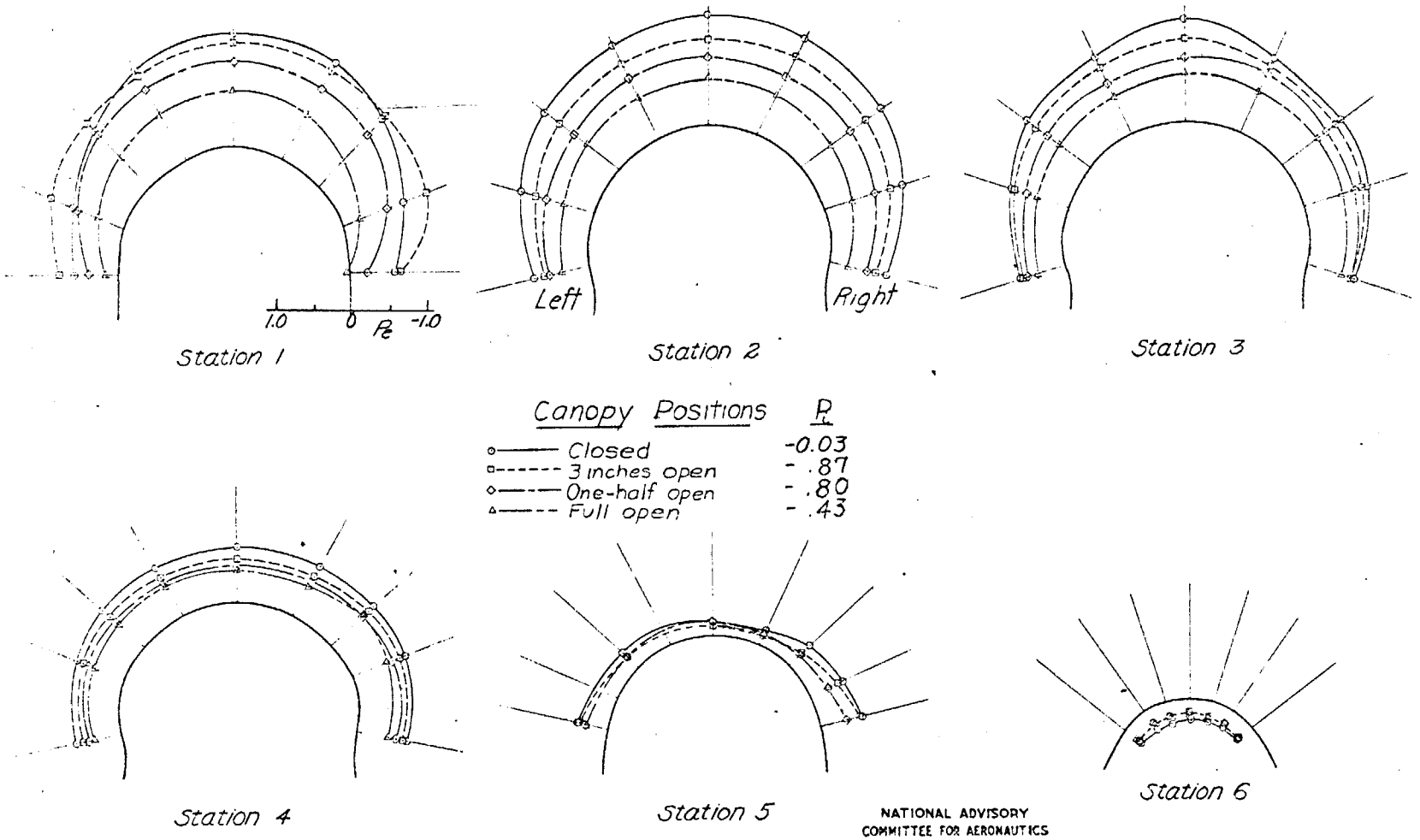

(c) Military power; T_c, 0.34; C_L, 0.87

Figure 10.-Continued.

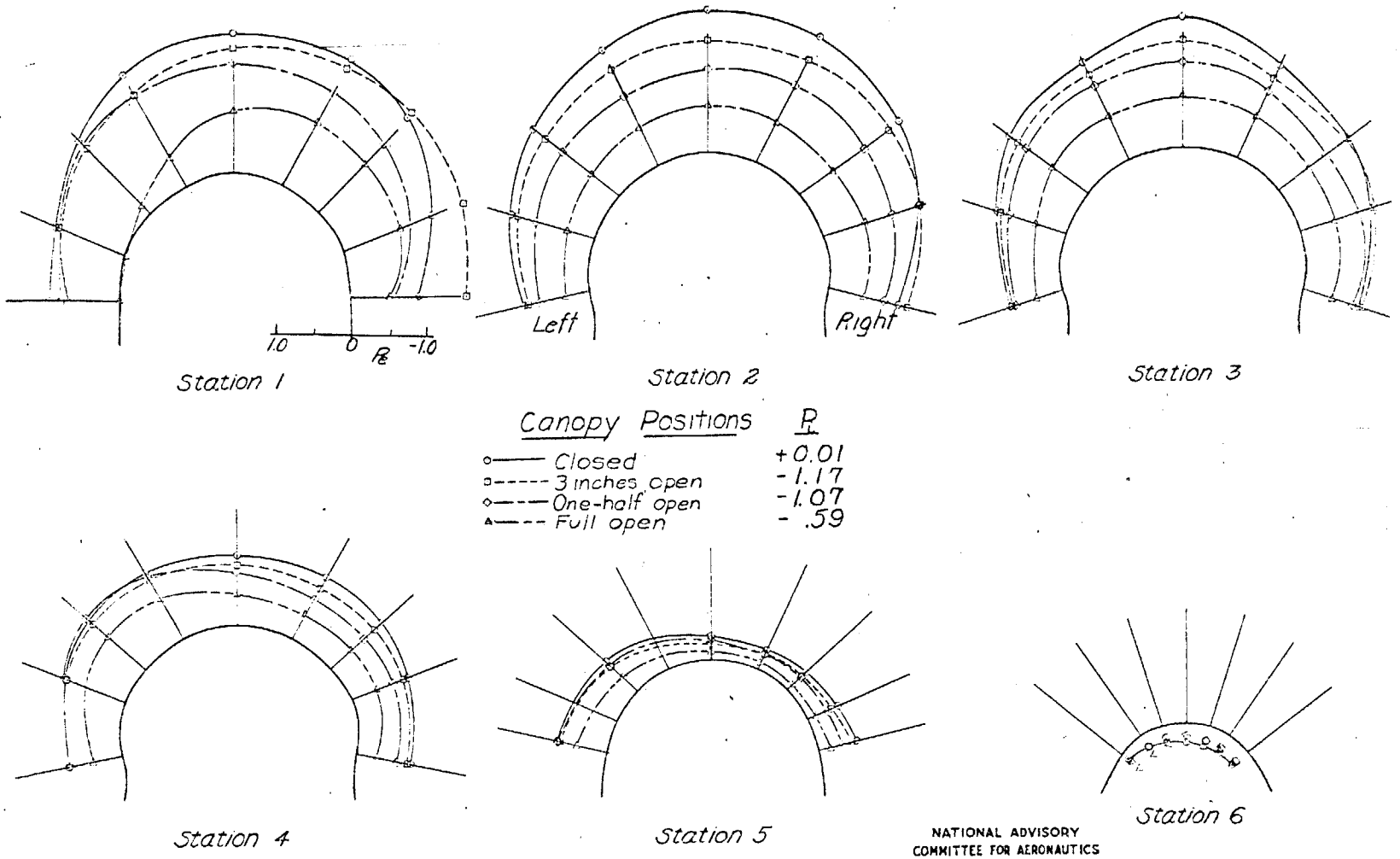

(d) Military power: T_c, 0.48, C_L, 1.18

Figure 10.–Continued

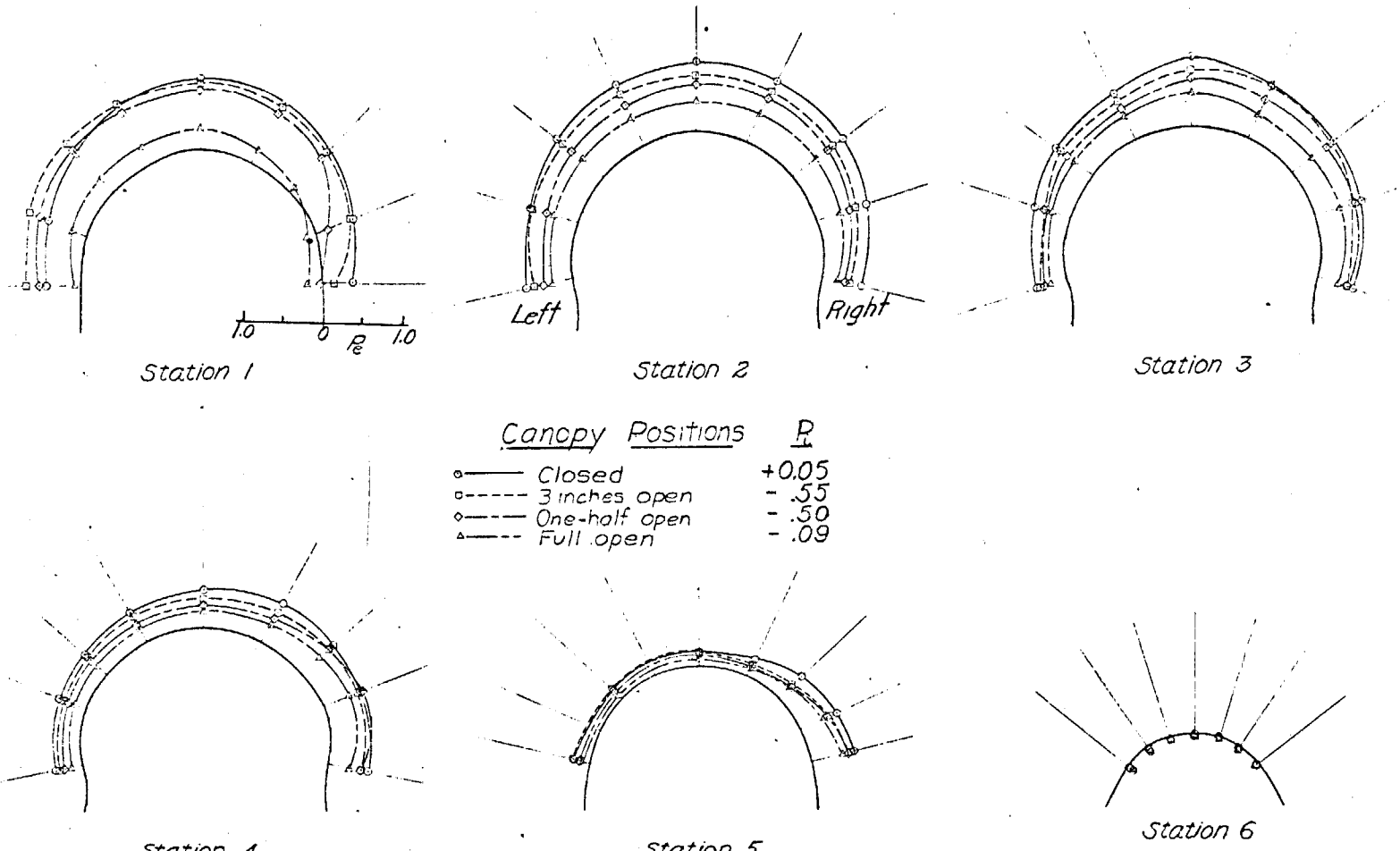

(e) Propeller idling; C_L, 1.18

Figure 10.-Concluded.

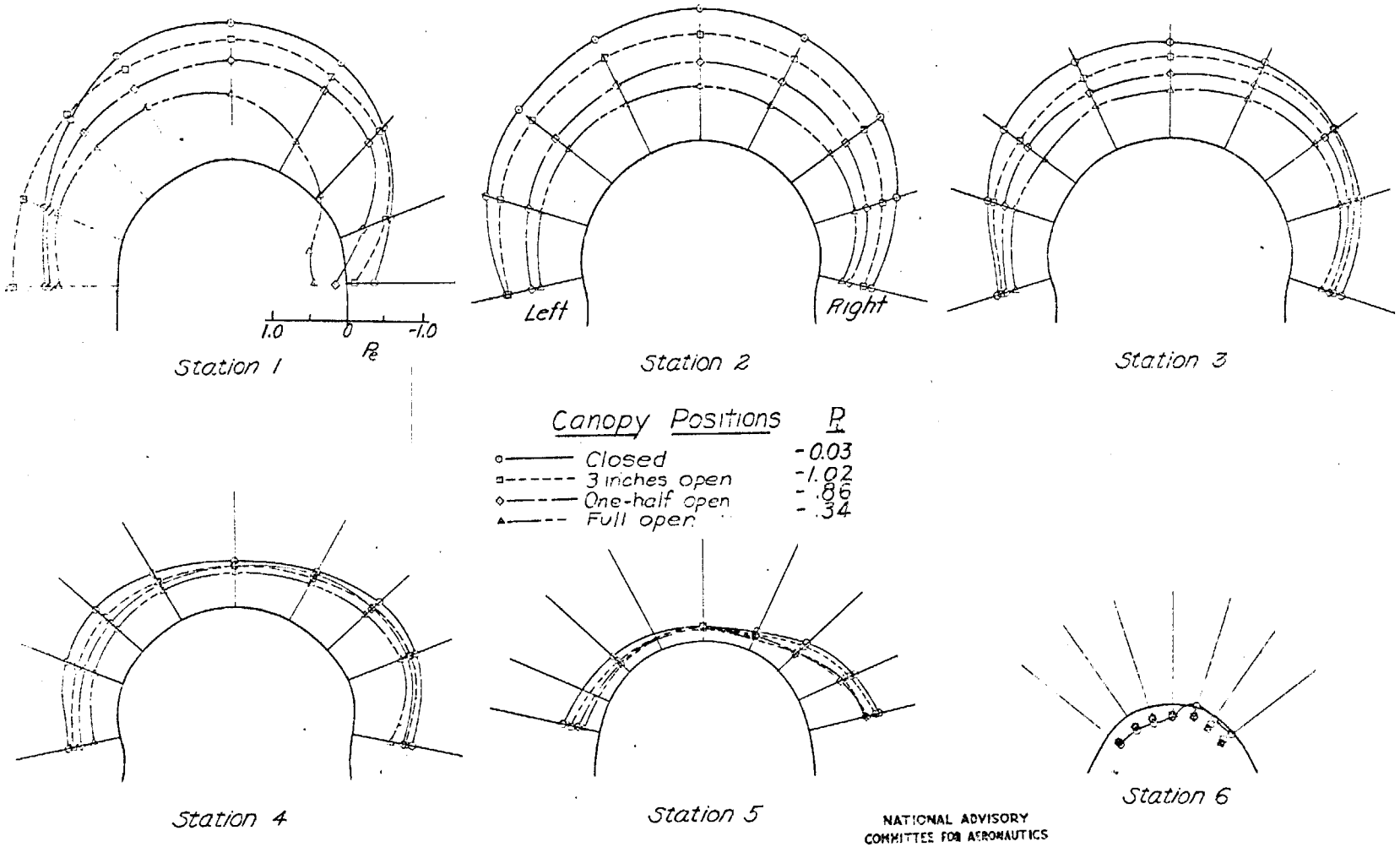

(a) Military power; T_c, 0.34; C_L, 0.87

Figure 11.-Pressure distributions over the canopy of the F8F-1 airplane. γ, -15°

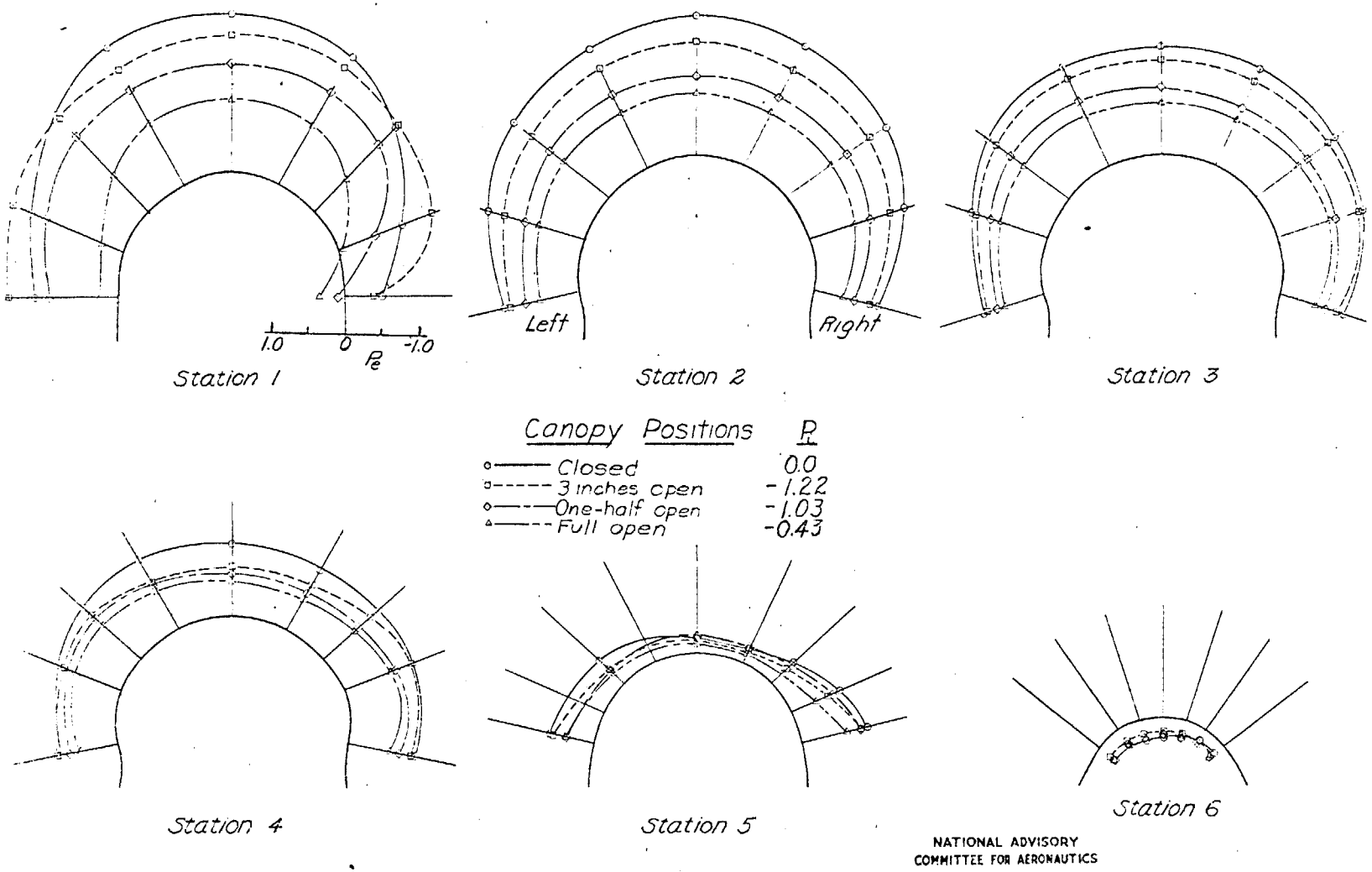

(b) Military power; T_c .048; C_L 1.18

Figure 11.—Continued.

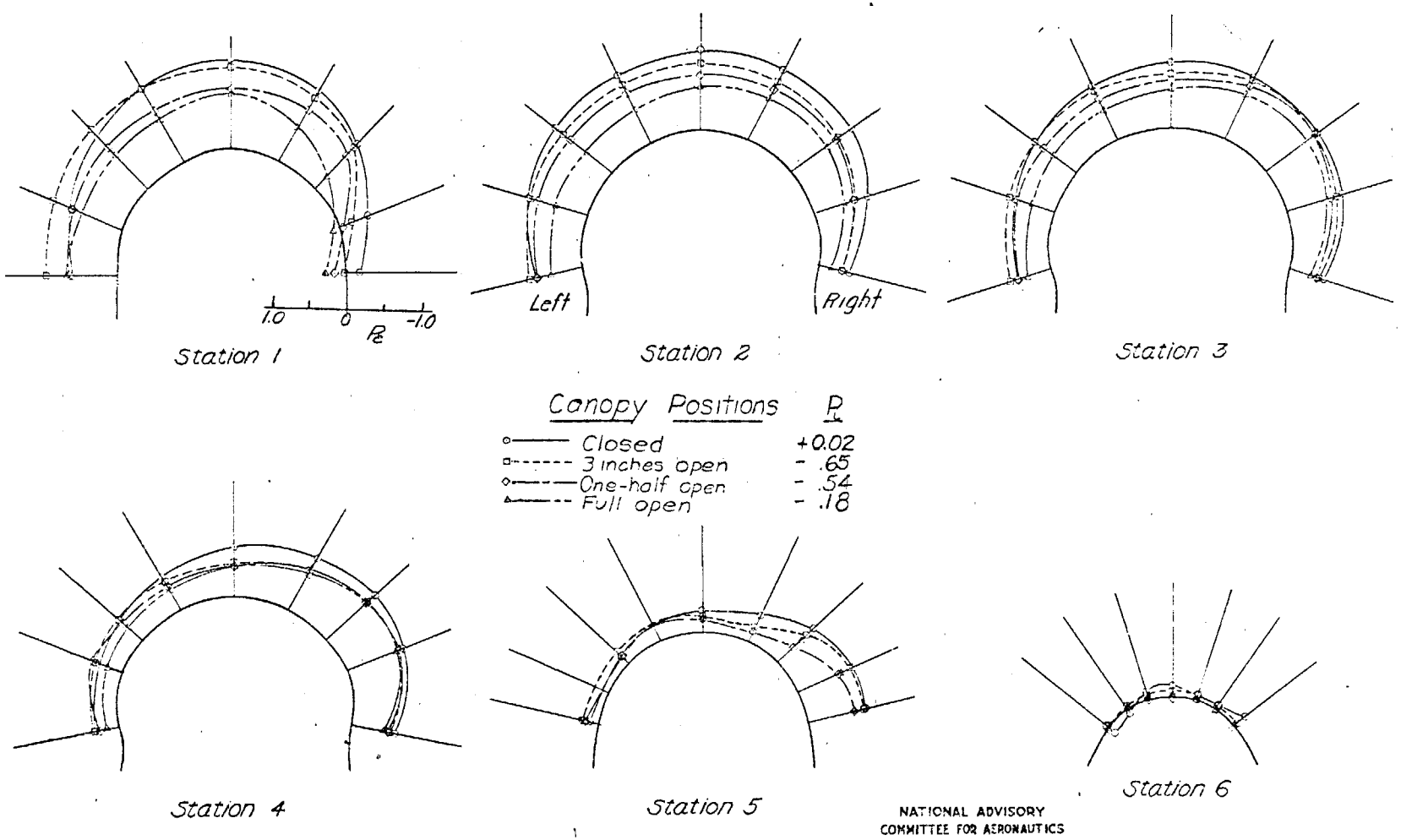

(c) Propeller idling; C_L, 1.18

Figure 11.-Concluded.

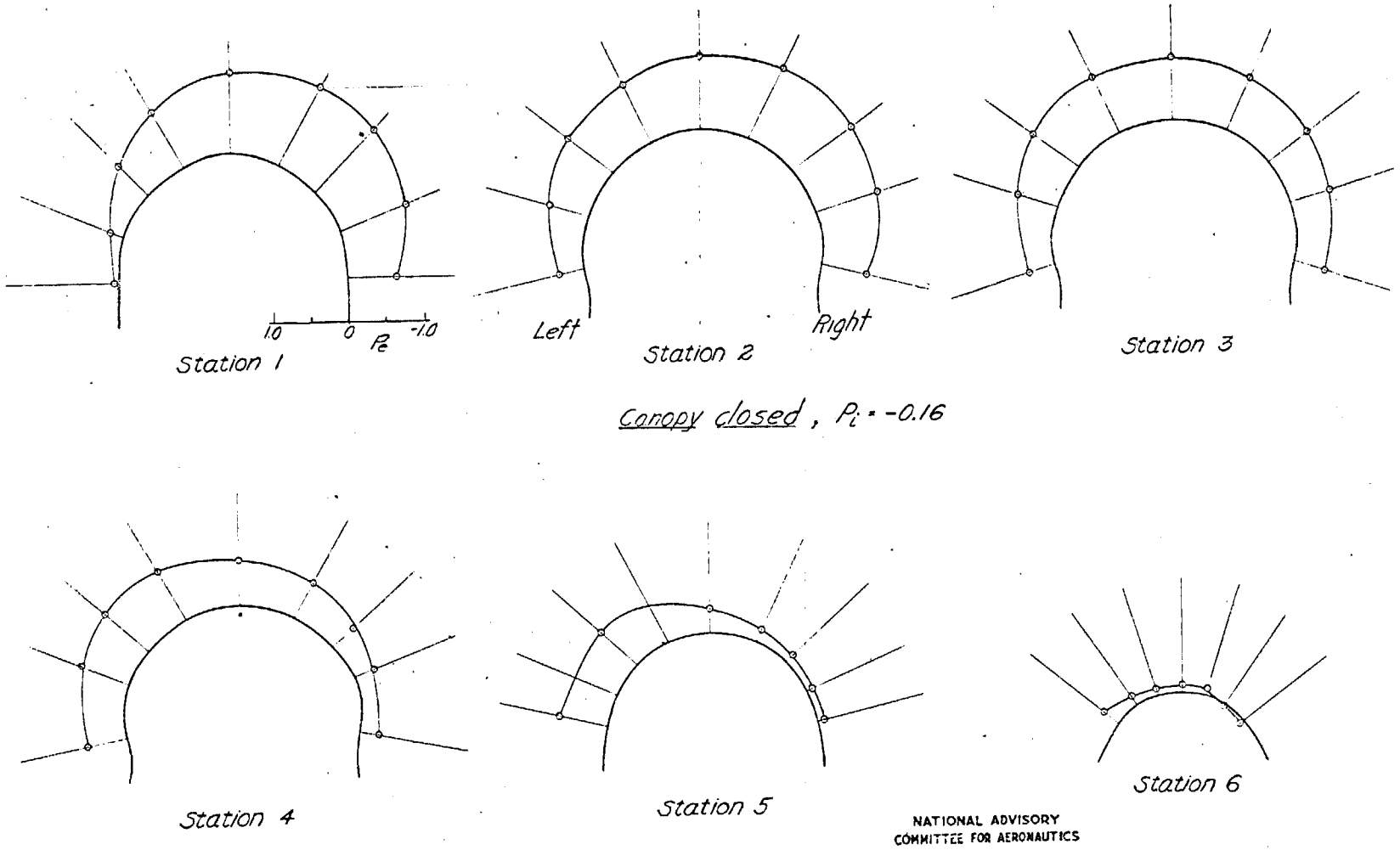

Canopy closed, $P_i = -0.16$

(a) Military power; T_c, .002; C_L, 0.10

Figure 12.-Pressure distributions over the canopy of the F8F-1 airplane. χ, 7.5

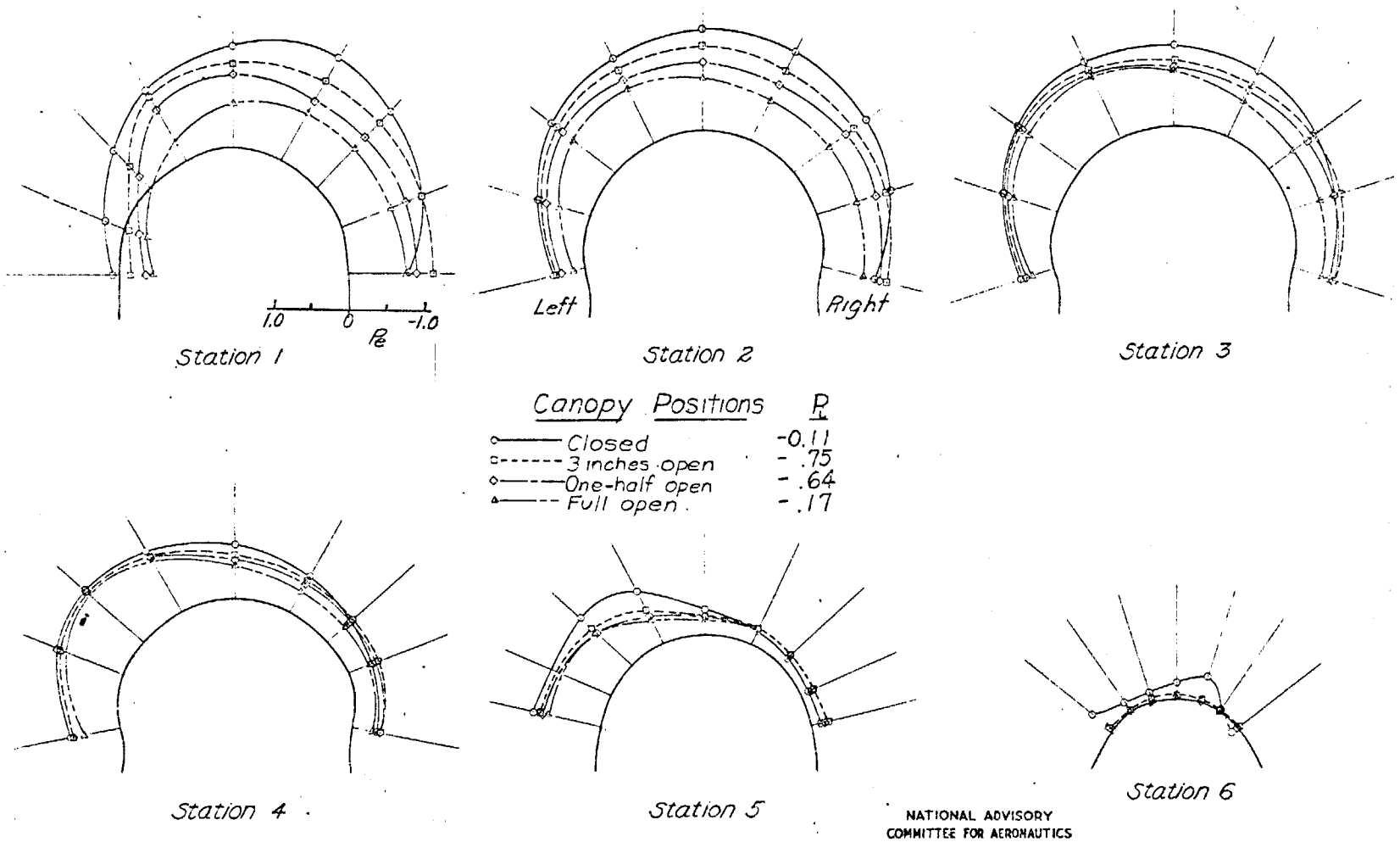

(b) Military power; T_c,017; C_L,0.50

Figure 12.-Continued.

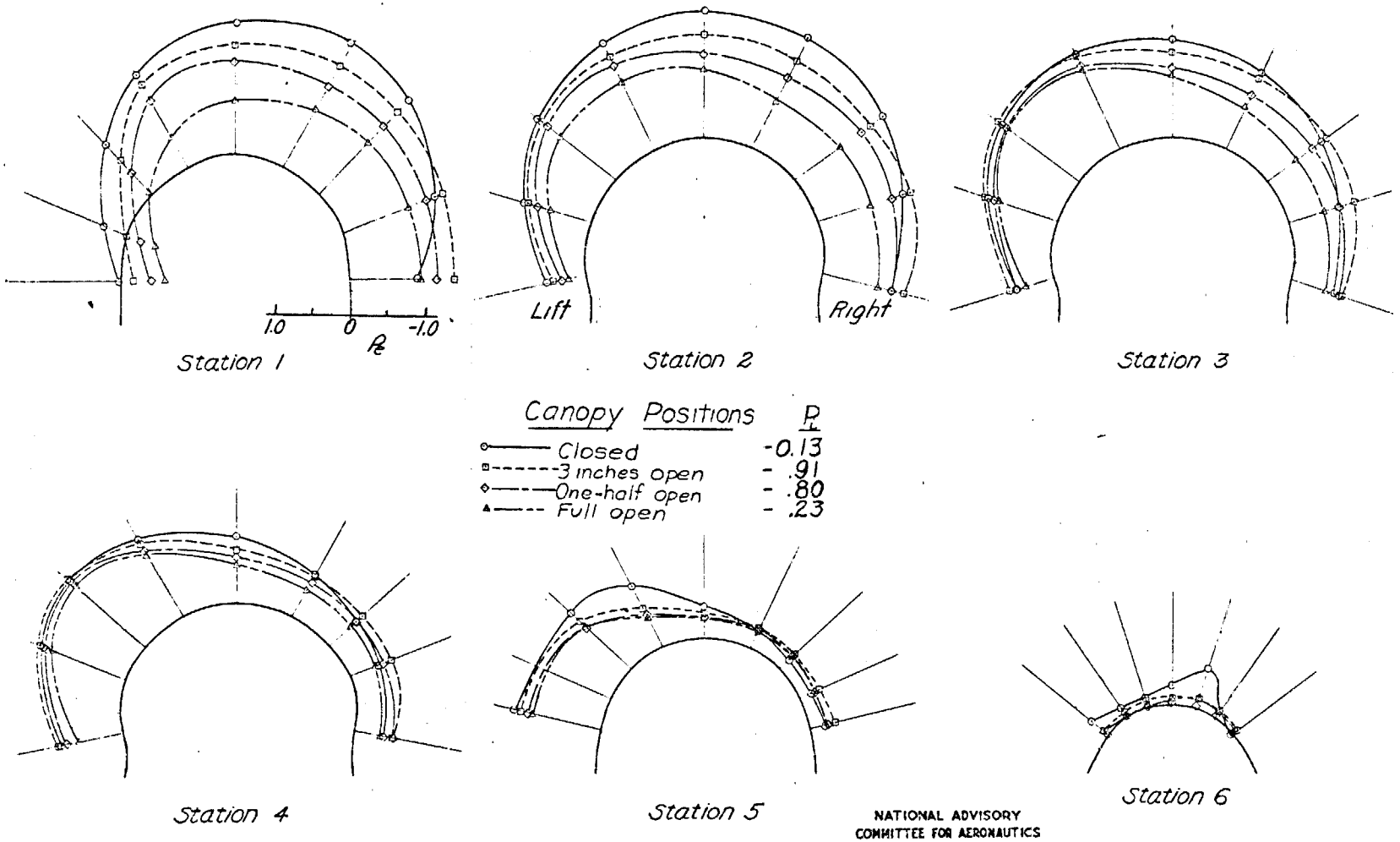

(c) Military power; T_c, 0.34; C_L, 0.87

Figure 12.-Continued.

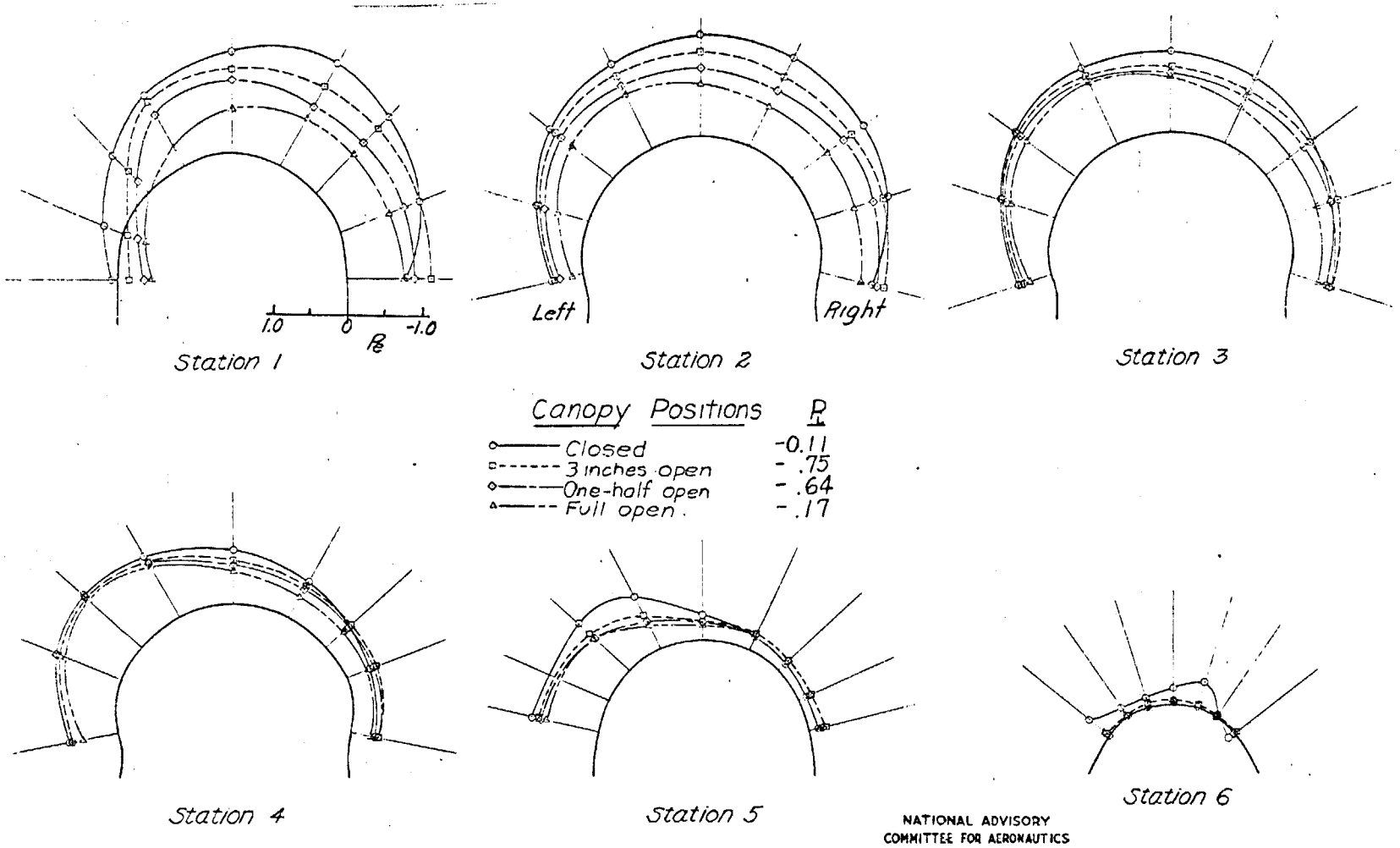

(b) Military power; T_c, 0.17; C_L, 0.50

Figure 12.-Continued.

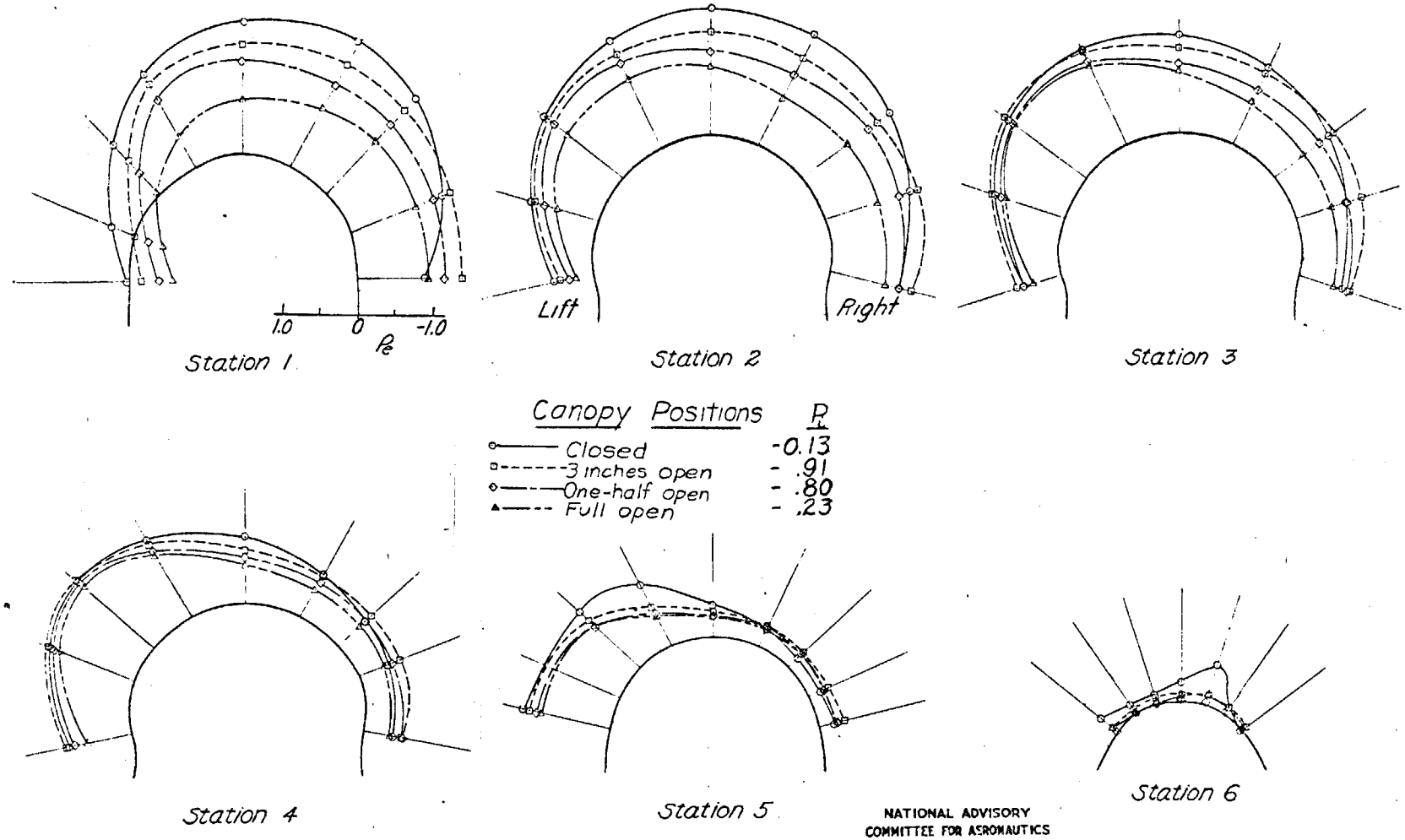

(C) Military power; T_c, 0.34; C_L, 0.87

Figure 12.-Continued.

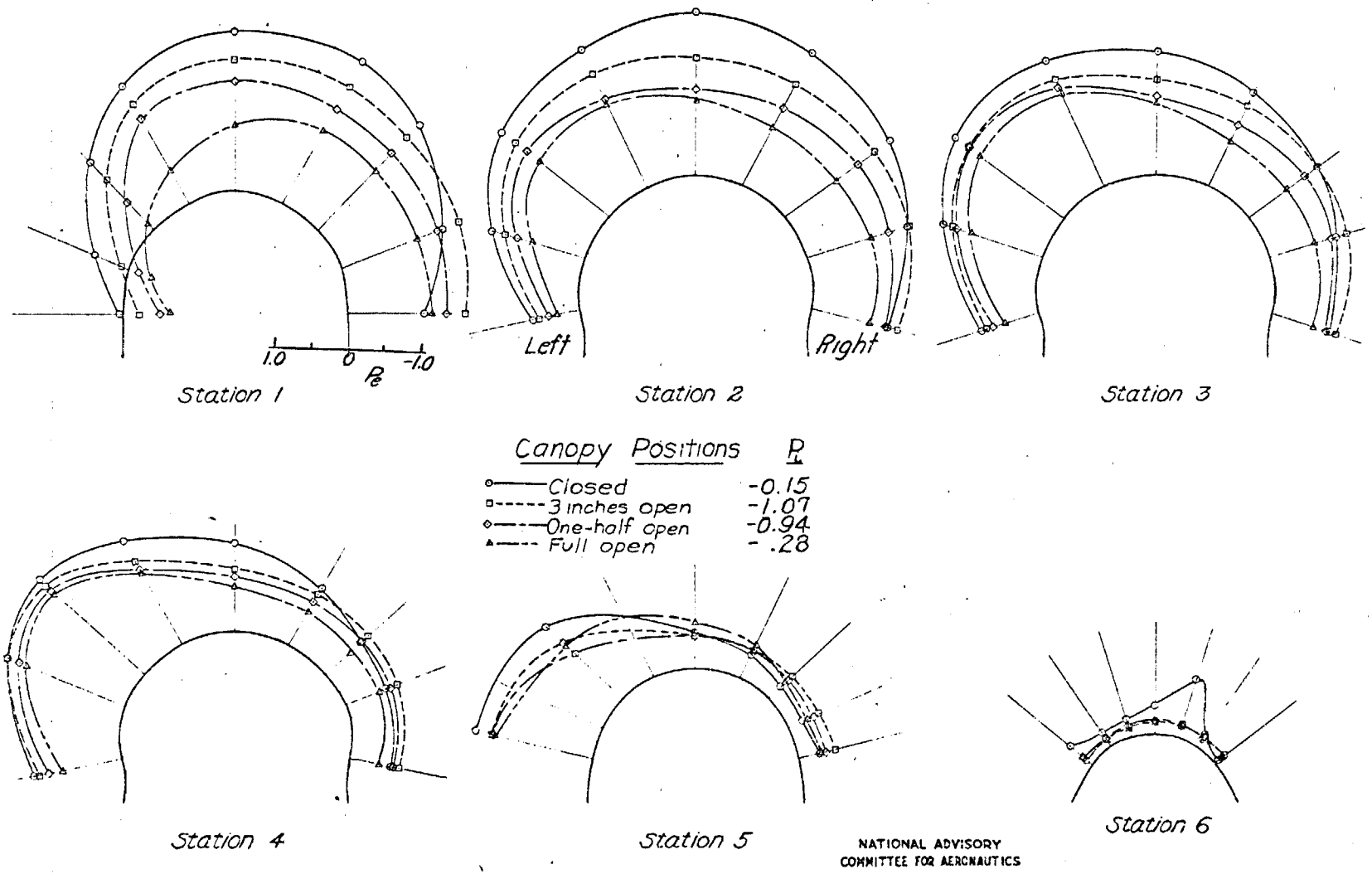

(d) Military power; T_c, .048; C_L, 1.18

Figure 12.–Continued.

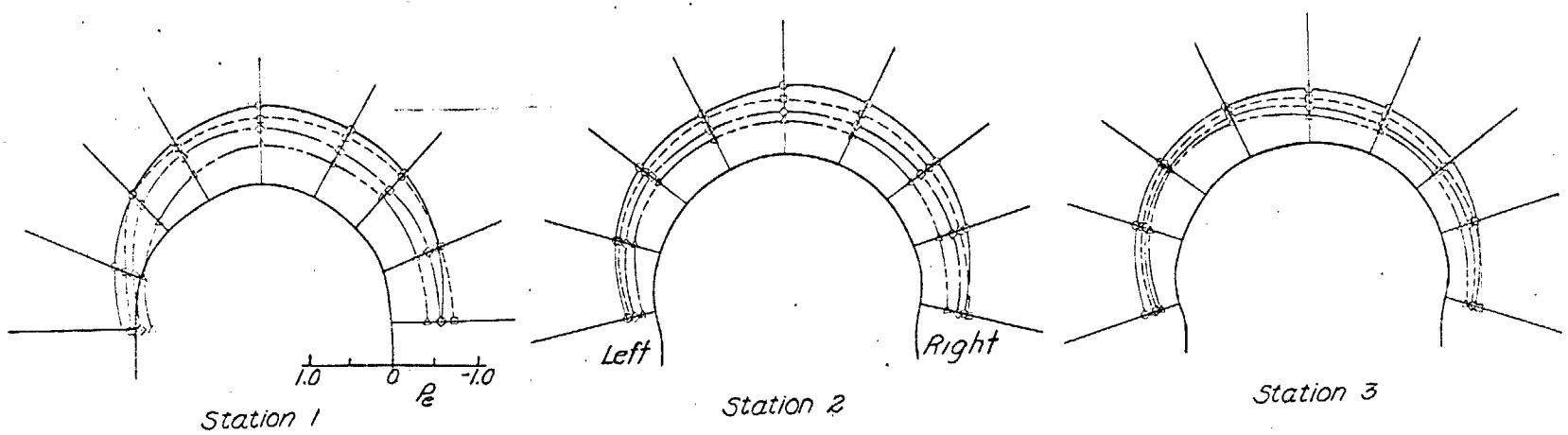

Station 1 Station 2 Station 3

Canopy Positions P_1

Closed	0.0
3 inches open	- .55
One-half open	- .46
Full open	- .16

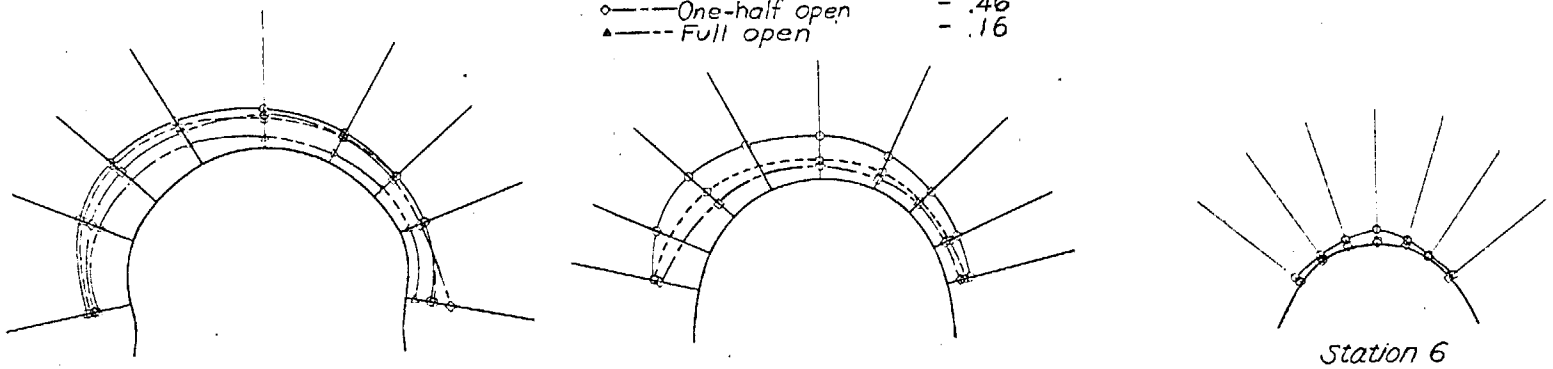

Station 4 Station 5 Station 6

(e) Propeller idling; C_L, 1.18

NATIONAL ADVISORY COMMITTEE FOR AERONAUTICS

Figure 12.- Concluded.

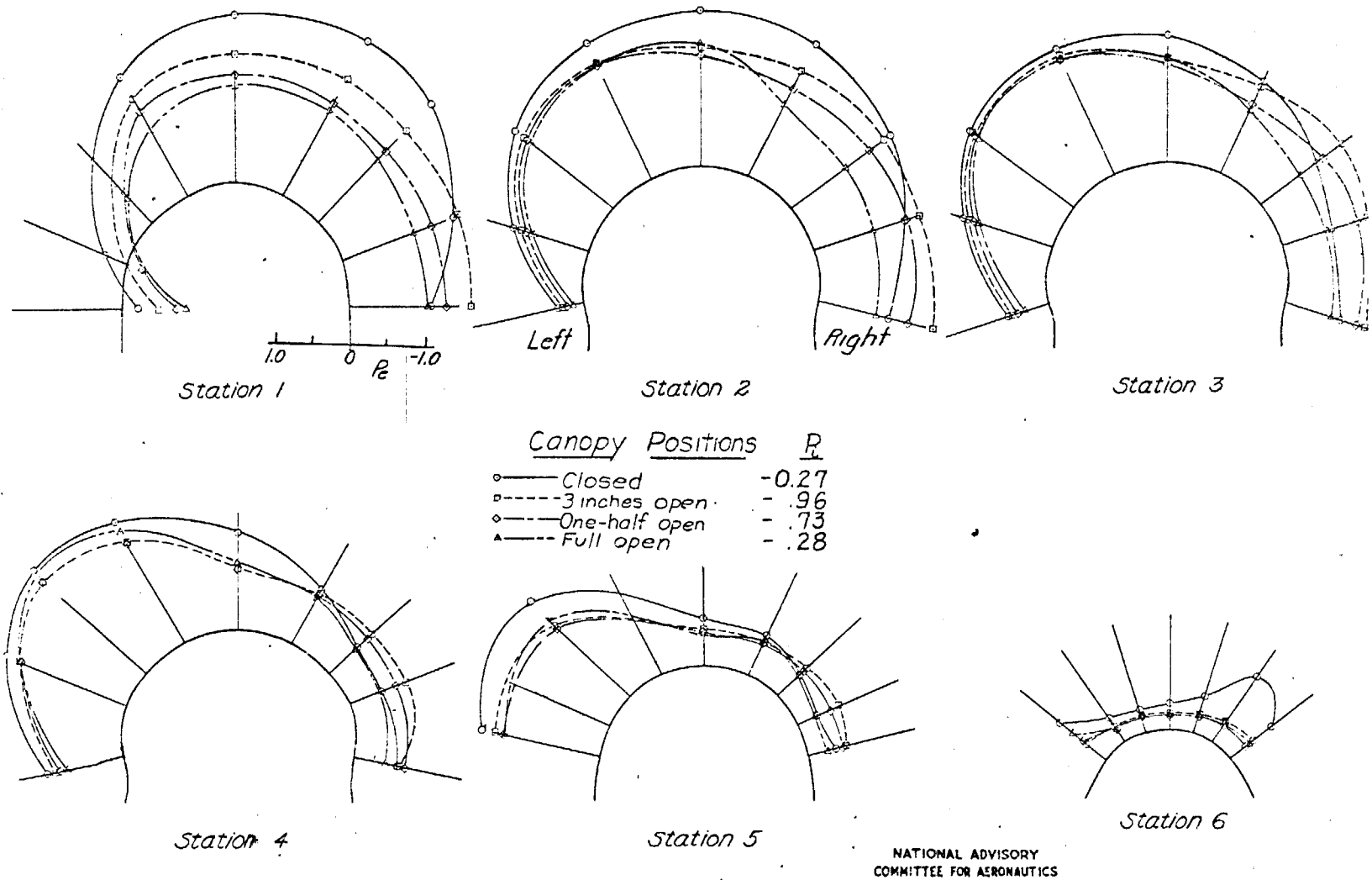

(a) Military power; T_c, 034; C_L, 0.87

Figure 13.- Pressure distributions over the canopy of the F8F-1 airplane. α, 15°.

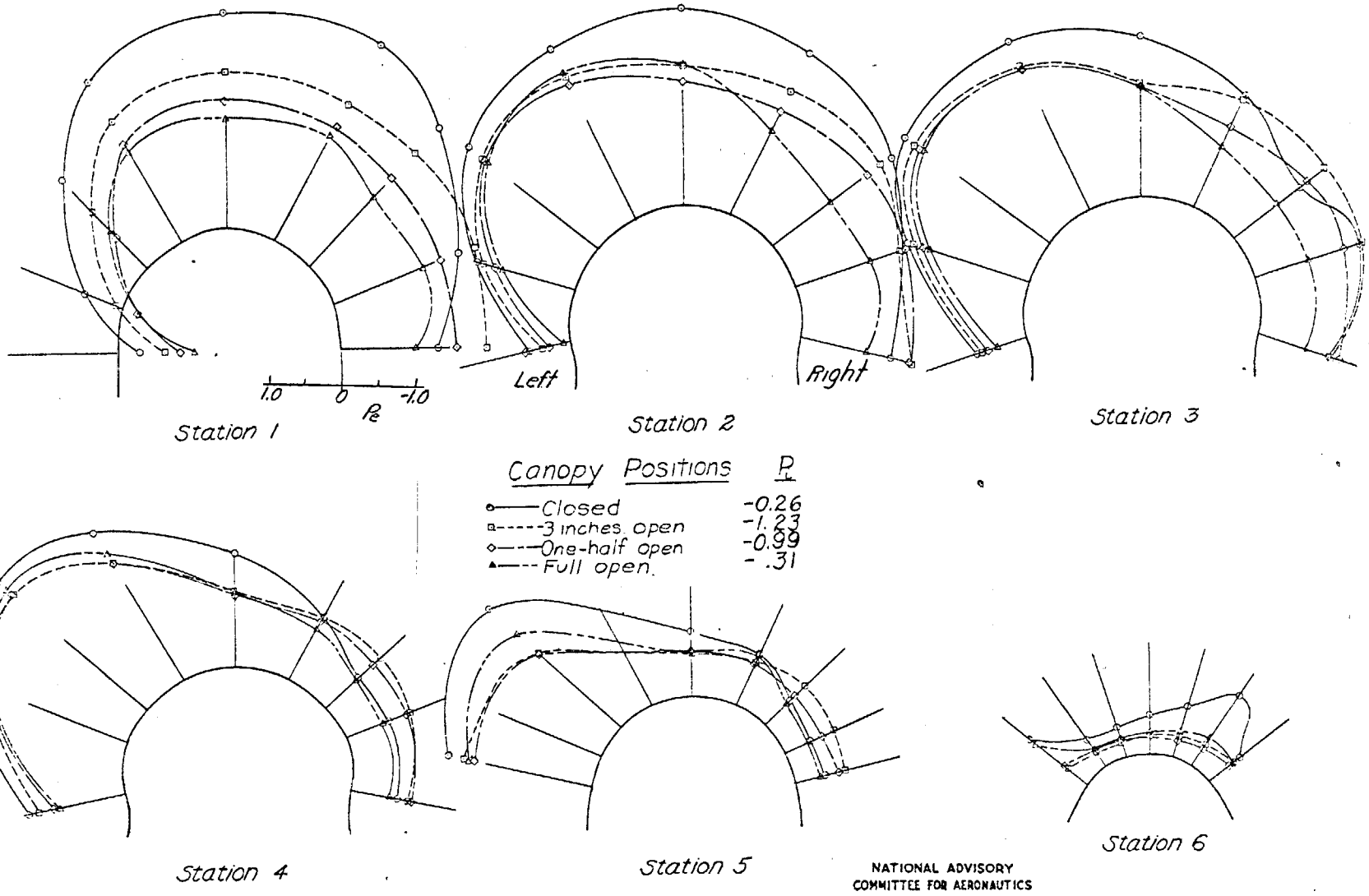

(b) Military power; T_c, 0.48; C_L, 1.18

Figure 13.—Continued.

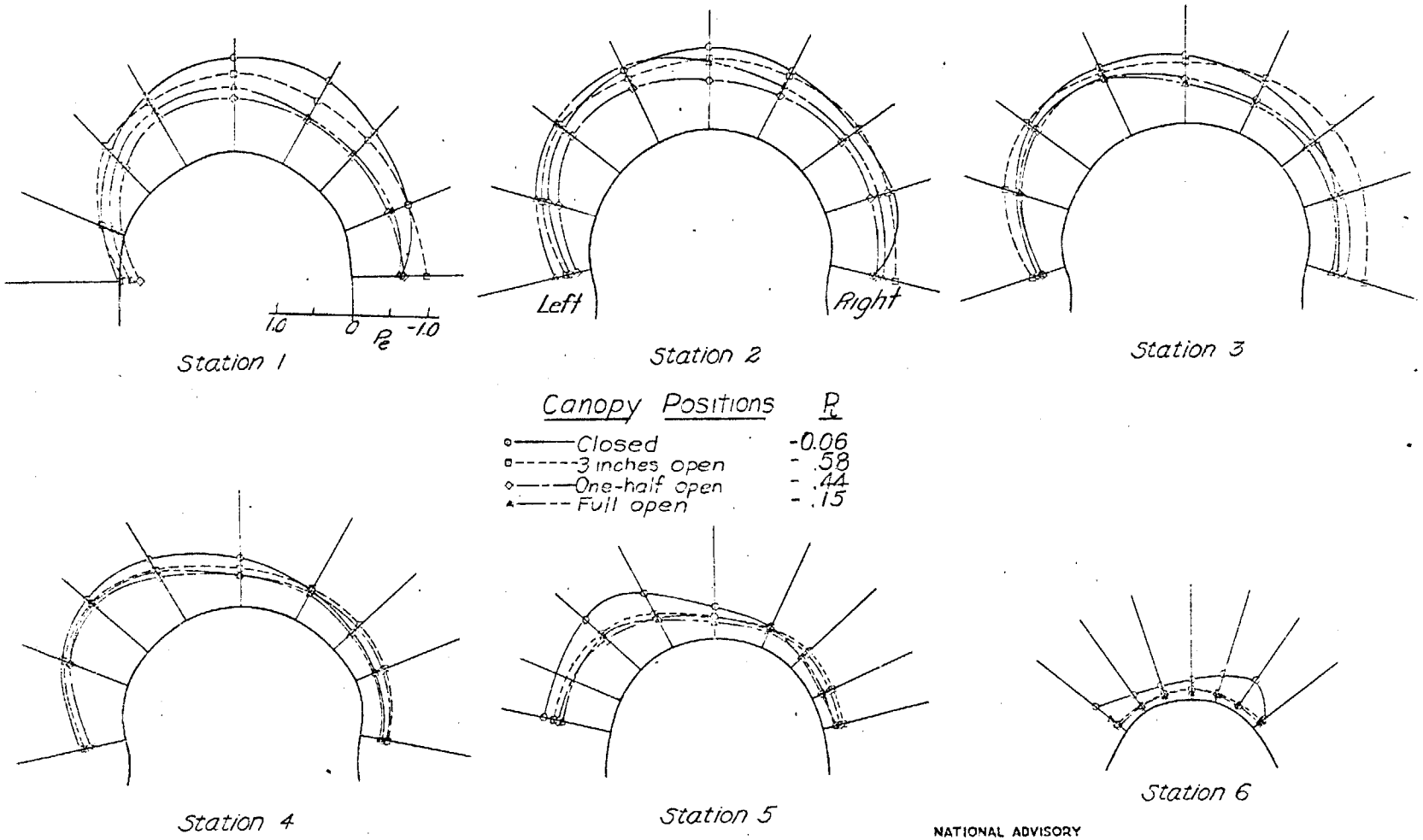

(c) Propeller idling; C_L, 1.18

Figure 13.-Concluded.

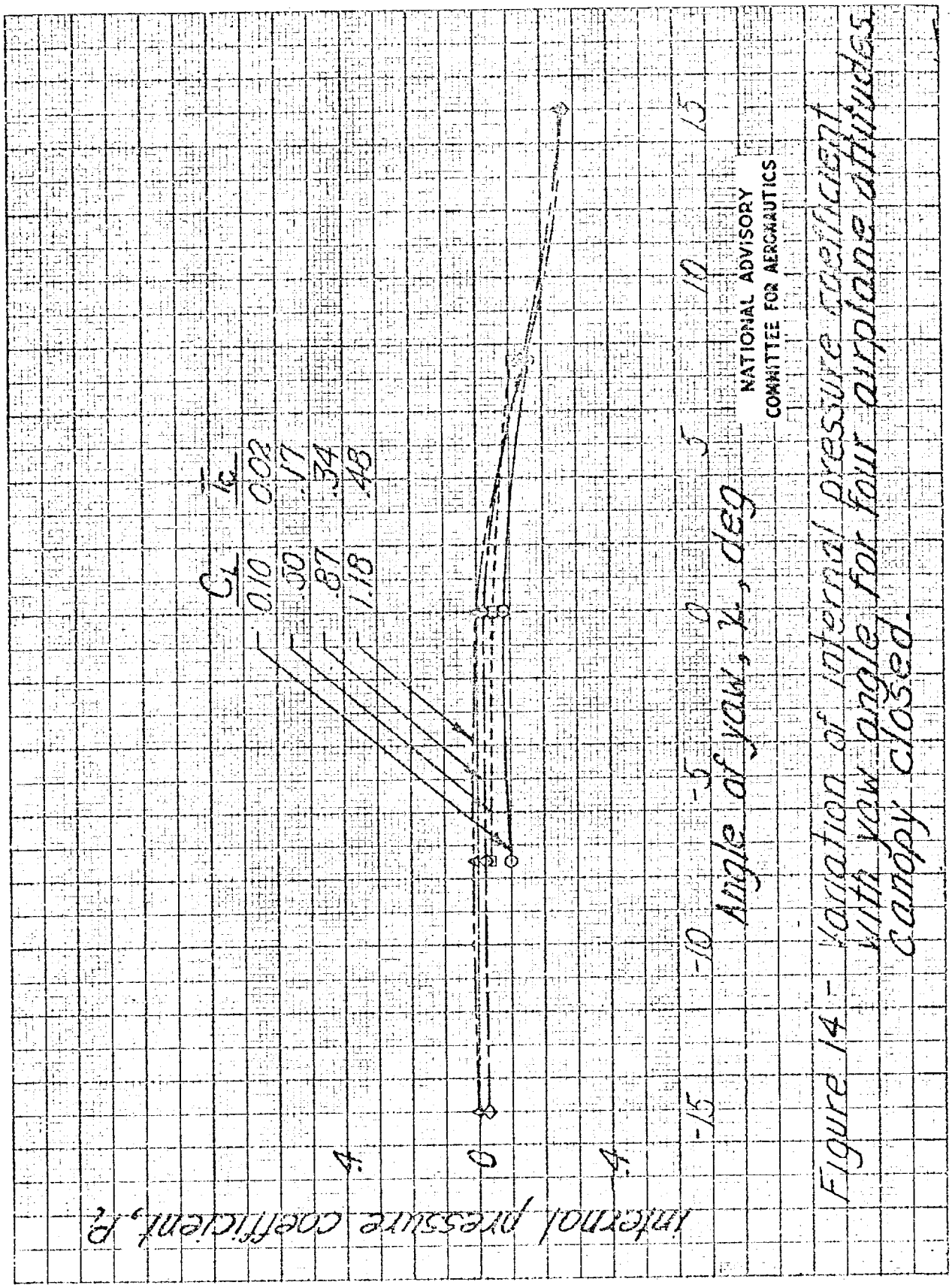

Figure 14 - Variation of internal pressure coefficient with yaw angle for four airplane attitudes. Canopy closed.